Medicinal Chemistry Research
https://doi.org/10.1007/s00044-020-02552-1

MEDICINAL CHEMISTRY RESEARCH

ORIGINAL RESEARCH

Cytotoxicity, anticancer, and antioxidant properties of mono and bis-naphthalimido β-lactam conjugates

Nassim Borazjani[1] · Maryam Behzadi[2] · Marzieh Dadkhah Aseman[3] · Aliasghar Jarrahpour[1] · Javad Ameri Rad[1] · Sedigheh Kianpour[2,4] · Aida Iraji[5] · S. Masoud Nabavizadeh[1] · Mohammad Mehdi Ghanbari[6] · Gyula Batta[7] · Edward Turos[8]

Received: 24 February 2020 / Accepted: 27 April 2020

Abstract

This article reports the diastereoselective synthesis of some novel naphthalimido and bis-naphthalimido β-lactam derivatives and a preliminary evaluation of their anticancer properties. The reactions were completely diastereoselective, leading exclusively to the formation of *cis*-β-lactams **11a–l** and *trans*-bis-β-lactams **16a–g**. All of these compounds were obtained in good to excellent yields and their structures were established based on IR, ^{1}H NMR, ^{13}C NMR spectral data, and elemental analysis. Each of the β-lactams was screened for antioxidant and anticancer activities. Our results showed that all the compounds lacked cytotoxicity against *HepG2* cells, whereas **16a** and **16b** exhibited excellent anticancer activity with IC_{50} values below 191.57 µM on *MCF-7* cell line and also, bis-β-lactams **16a–g** showed excellent antitumor activity against the *TC-1* cell line. Antioxidant experiments of **16a–d** by the diphenylpicrylhydrazyl (DPPH) assay showed IC_{50} values ranging from 7 to 32.3 µg/ml. Interaction of **16a**, **16b**, **16d–g** with calf-thymus DNA (CT-DNA) was also supported by absorption titration studies. The compounds exhibit good binding propensity to CT-DNA and the DNA binding affinity (K_b) of the compounds varies as **16a; 16b; 16e; 16g > 16d**; **16f**. Interaction of **16d** with CT-DNA was also investigated by fluorescence spectroscopy. The results support an intercalative interaction of **16d** and **16f** and non-intercalation mechanism for **16a**, **16b**, **16e,** and **16g**.

Keywords Anticancer · Antioxidant · Cytotoxicity · Diastereoselective · β-Lactam

Abbreviations

MCF-7	Breast cancer cells
TC-1	Mouse lung epithelial cells
HepG2	Liver hepatocellular carcinoma
DPPH	Diphenylpicrylhydrazyl
ORTEP	Oak Ridge Thermal Ellipsoid Plot
CT-DNA	Calf thymus-deoxyribonucleic acid
K_b	binding affinity
IC50	Half maximal inhibitory concentration
NI	Naphthalimide
NDI	1,4,5,8-Naphthalenetetracarboxylicdiimide
MTT	Methyl thiazol tetrazolium bromide
OD	Optical density

Supplementary information The online version of this article (https://doi.org/10.1007/s00044-020-02552-1) contains supplementary material, which is available to authorized users.

✉ Aliasghar Jarrahpour
jarahpor@shirazu.ac.ir

[1] Department of Chemistry, College of Sciences, Shiraz University, Shiraz 71946-84795 I.R., Iran

[2] Pharmaceutical Research Center, Shiraz University of Medical Sciences, Shiraz, Iran

[3] Department of Chemistry, Kharazmi University, Tehran 1983969411, Iran

[4] Biotechnology Research Center, Shiraz University of Medical Sciences, Shiraz, Iran

[5] Central Research Laboratory, Shiraz University of Medical Sciences, Shiraz, Iran

[6] Department of Chemistry,Sarvestan Branch, Islamic Azad University, Sarvestan, Iran

[7] Department of Chemistry, University of Debrecen, Debrecen Egyetem tér 1, Debrecen 4032, Hungary

[8] Center for Molecular Diversity in Drug Design, Discovery, and Delivery, Department of Chemistry, University of South Florida, CHE 205, 4202 East Fowler Avenue, Tampa, FL 33620, USA

Published online: 10 May 2020

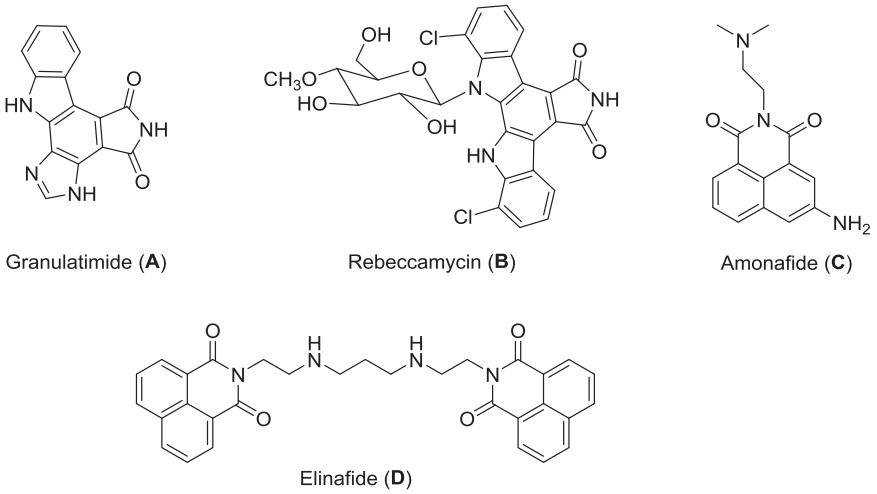

Fig. 1 Structures of biologically-active cyclic imides and selected DNA-intercalating agents

Introduction

Cancer is a collection of diseases characterized by abnormal cell growth and the possibility of attacking other parts of the body. In 2015, the World Health Organization reported the five most common cancer deaths worldwide, including liver cancer, colorectal cancer, lung cancer, breast cancer, and gastric cancer (Miller et al. 2016). Although a plethora of anticancer drugs are commercially available, most have serious side effects. In addition, there is an urgent need to discover and to synthesize new anticancer drugs (Kumar et al. 2017). The imide moiety is an integral part of the structures of some of the most important anticancer drugs, such as uramustine (Baraldi et al. 2002), granulatimide **A** (Berlinck et al. 1998), and rebeccamycin **B** (Zhang et al. 2005) (Fig. 1). Cyclic imide derivatives have a wide range of biological activities such as antimicrobial (Anizon et al. 1997), antitumor (Henon et al. 2007; Laronze et al. 2005), anti-inflammatory activity (Amr et al. 2007), antioxidative and anticonvulsant activities (Abdel-Aziz et al. 2011; Machado et al. 2011; El-Azab et al. 2013), and serve as inhibitors of *N*-aminopeptidase (Li et al. 2010) and *Mycobacterium tuberculosis* protein tyrosine phosphatase B (De Oliveira et al. 2011). Bis cyclic imides likewise have anti-inflammatory, anticancer, analgesic, and anticoagulant activities (Arya et al. 2013; Said et al. 2009). Naphthalimide (NI) and 1,4,5,8-naphthalenetetracarboxylic diimide (NDI) act as duplex DNA intercalators and have shown anticancer activity against several human cancer cell lines. DNA is the carrier of genetic information involved in gene expression, protein synthesis, and cell growth and division. As a result, DNA is highly regarded as an important target for the design of new anticancer drugs. Many compounds exert anticancer effects through binding to duplex DNA, through three general modes: (1) interactions with the anionic phosphates in the DNA backbone, (2) interactions with the major or minor grooves of DNA, and (3) intercalation between stacked base pairs (Tomczyk and Walczak 2018). Two examples of DNA-intercalating agents, amonafide **C** and elinafide **D** (Fig. 1), were initially identified as having promising anticancer properties but did not pass Phase II trials due to elevated toxicity. Several attempts have been made to overcome this limitation by synthesizing various analogues (Ge et al. 2017; Tumiatti et al. 2009). 1,8-Naphthalimide derivatives such as **C** and **D** are also known for their strong fluorescence properties and are used as pigments in polymer industries, fluorescent probes for biological purposes and medical, DNA fragmentation factors, crystalline liquid additions, potential anti-HIV drugs, and laser colors (Xiao et al. 2010).

The β-lactam antibiotics, most notably the penicillins, cephalosporins, monobactams, and the penicillinase inhibitor, clavulanic acid, has led to worldwide applications toward the control of infectious bacterial diseases. Besides their recognized antibacterial properties, β-lactams are also known for an even wider range of biological activities such as anticancer, anti-inflammatory, antimalarial, and antitubercular. β-Lactams have also been used as prodrugs to deliver cancer chemotherapeutic agents directly to a tumor site (Geesala et al. 2016) and as synthetic building blocks. β-Lactam derivatives have been also reported to increase DNA damage and lead to apoptosis of T cells in human leukemia cells. Interestingly, one of the β-lactams has inhibited cell proliferation and has induced apoptosis in several tumor cell lines (Arya et al. 2014; Parul et al. 2010; Galletti et al. 2014). An emerging strategy in drug discovery campaigns is that of the pharmacophore hybridization, in which two independently bioactive moieties are covalently joined into a single molecular unit. Some examples include antibacterial hybrid **E** (Borazjani et al. 2019a, 2019b), anticancer hybrid **F** (Borazjani et al. 2019a, 2019b), anti-inflammatory hybrid **G** (Borazjani et al. 2019a, 2019b), and

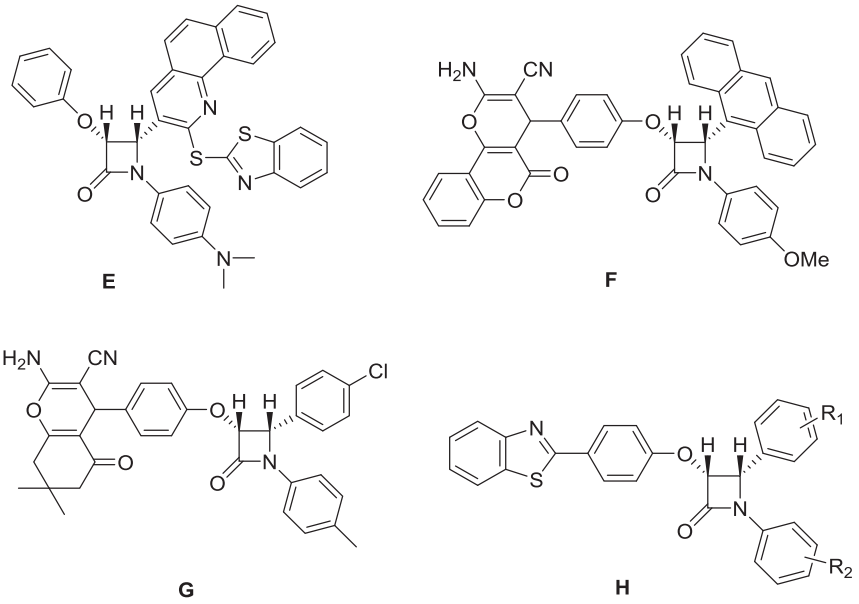

Fig. 2 Examples of hybrid compounds with antibacterial, anticancer, anti-inflammatory and antimalarial activity

antimalarial hybrid **H** (Alborz et al. 2018) (Fig. 2). Important motivations for expanding upon this concept include the creation of new chemical constructs with enhanced biological activity that can circumvent drug resistance or the use of active transport mechanisms that add therapeutic value in terms of potency, breadth of bioactivity, improved pharmacokinetics, or delay in the onset of drug resistance (Baraldi et al. 2007; Wang et al. 2012). Therefore, we decided to use the molecular hybridization strategy by exploiting the rich chemistry and known biological effectiveness of β-lactams and 1,8-naphthalimides. In addition to synthesizing representative structures, we also were interested in studying their anticancer and antioxidant activities as well as potential cytotoxicity.

Results and discussion

Chemistry

In this study, twelve novel naphthalimido *cis*-β-lactams **11a–l** were synthesized by the Staudinger reaction of one of three *N*-aryl imines **9a–c** with various aryloxyacetic acids **10a–d**, shown in Scheme 1 (Palomo et al. 2004). In the first step, 1,8-naphthalimide (**3**) was prepared in 95% yield by the reaction of commercially-available 1,8-naphthalic anhydride (**1**) and ammonium acetate (**2**) at 60 °C using DMF as solvent. Then, a mixture of 1,8-naphthalimide **3**, 1,3-dibromopropane (**4**) and K_2CO_3 stirred together in DMF at room temperature afforded bromo-*N*-propyl-1,8-naphthalimide (**5**) in 90% yield (Kamal et al. 2002). Recrystallized compound **5** was treated with 4-hydroxybenzaldehyde (**6**) in the presence of K_2CO_3 in acetonitrile to afford 4-(3-(1,3-dioxo-1*H*-benzo[*de*]isoquinolin-2(3*H*)-yl)propoxy)benzaldehyde (**7**) in 95% yield. The structure of compound **7** was characterized by IR, ^{1}H NMR, and ^{13}C NMR spectroscopy and elemental analysis data. For example, the IR spectrum of **7** showed the characteristic stretching absorption for the aldehyde carbonyl at 1674 cm^{-1} and twin absorption bands for the naphthalimide carbonyl groups at 1699 and 1657 cm^{-1}. The ^{1}H NMR spectrum of compound **7** exhibited a singlet at δ 9.82 for the aldehyde proton, as well as all the expected resonances for the other protons. The ^{13}C NMR spectral data for compound **7** gave a signal at δ 191.2 for the aldehyde carbon.

Aldehyde 7, when treated with aniline derivatives **8a–c** in ethanol, readily afforded the corresponding *N*-aryl imines **9a–c**. The IR spectrum of **9a** shows the expected absorption for the imine (CH=N) at 1624 cm^{-1} and absorption bands for the naphthalimide carbonyl groups at 1696 and 1659 cm^{-1}. The ^{1}H NMR spectrum of **9a** displayed a signal at δ 8.43 corresponding to the imine proton (CH=N). Imines **9a–c** were then subsequently reacted with various phenoxyacetic acid derivatives **10a–d** in the presence of triethylamine and tosyl chloride, in molar ratios of 1:1.5:5:1.5, in anhydrous CH_2Cl_2 (Scheme 1). These reactions led to the stereoselective formation of naphthalimido *cis*-β-lactams **11a–l** in good to excellent yields (75–95%, Table 1).

These cycloaddition reactions were totally diastereoselective and afforded the *cis* stereoisomers as the only products, as an unresolved racemic mixture. The structures of β-lactams 11**a–l** were characterized by elemental analysis and IR, ^{1}H NMR, and ^{13}C NMR spectroscopy. As a representative example, the IR spectrum of **11a** showed the characteristic absorption of a sharp band of β-lactam carbonyl at 1751 cm^{-1}. The C=O absorption band of

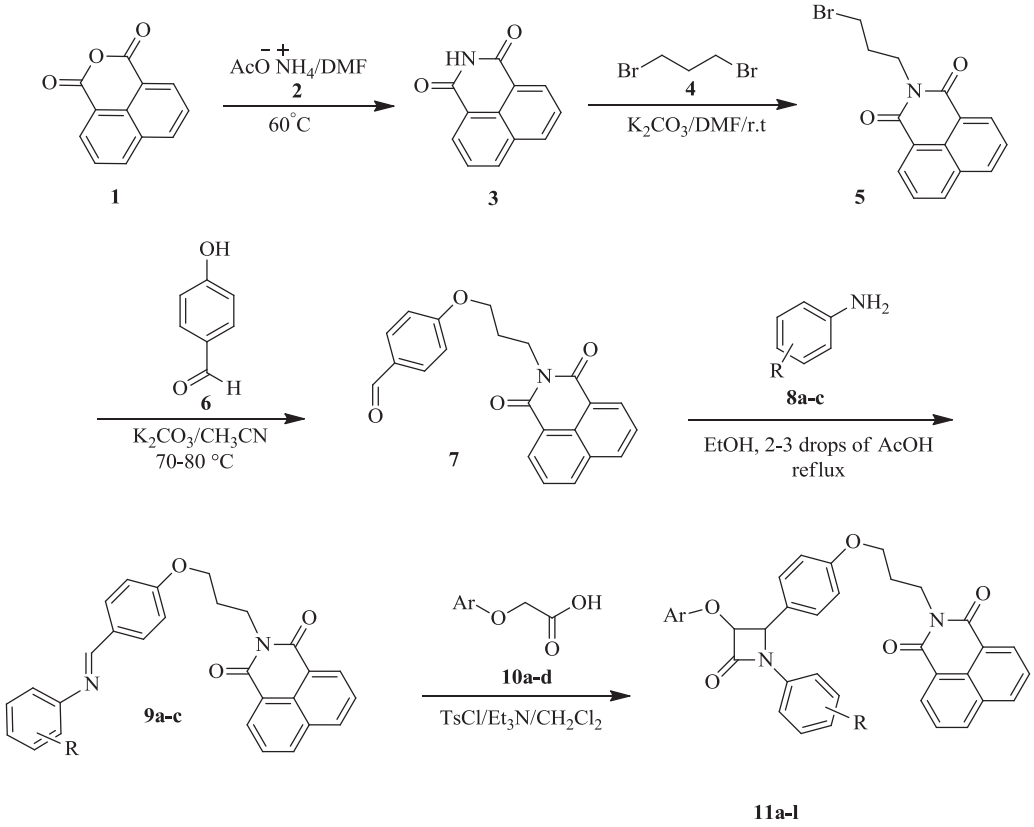

Scheme 1 Synthesis of naphthalimido *cis*-β-lactams **11a–l**

naphthalimide carbonyl groups appeared at 1697 and 1658 cm^{-1}. The *cis* stereochemistry of **11a** was deduced readily from the ^{1}H NMR spectrum, by the *β*-lactam ring's proton H-4 showing up as a doublet at δ 5.59 with $J =$ 4.7 Hz and H-3 appearing as a doublet at δ 5.76 with $J =$ 4.7 Hz (Fig. 3). ($J_{3,4} < 3.0$ Hz for the *trans* and $J_{3,4} > 4.0$ Hz for the *cis* stereoisomer) (Ameri Rad et al. 2017). The IR, ^{1}H NMR, and ^{13}C NMR spectroscopic data of compounds **11a–l** are presented in the supporting information.

Single crystal X-ray analysis of β-lactam **11b** confirmed the *cis* stereochemistry (Fig. 4). Crystallographic data, details of the data collection, and structure refinement can be found in the supporting information (Westrip 2010).

Next we turned to preparation of bis-β-lactams **16a–g** built from naphthalenetetracarboxylic diimide (**14**), which we synthesized from commercial 1,4,5,8-naphthalenetetracarboxylic dianhydride (**12**). We note that naphthalenetetracarboxylic diimide derivatives have previously been used as semiconductors due to the easy addition of varied substituents to the imide moiety, as a means to exert electronic effects and increase the efficiency of electron absorption (Gudeika et al. 2012). Compound **12** reacted with glycine (**13**) in DMF to afford naphthalenetetracarboxylic diacetic acid (**14**). Then, compound **14** was treated with different aromatic imines **15a–g** in the presence of triethylamine and p-toluenesulfonyl in anhydrous dichloromethane to afford bis-naphthalimido β-lactams **16a–g** in 40–68% yields (Scheme 2).

The structures of the bis-cycloaddition products were characterized by IR, ^{1}H NMR, ^{13}C NMR spectral data, and elemental analysis data (see Supplementary Information). As an illustration, the IR spectrum of bis-β-lactam **16e** showed a sharp β-lactam C=O absorption band centered at 1759 cm^{-1}, as well as twin C=O absorption bands for the naphthalimide carbonyl groups at 1712 and 1674 cm^{-1}. The ^{1}H NMR spectrum of **16e** exhibited separate doublets at δ 5.42 and 5.94 for the vicinal protons on each β-lactam ring, whose coupling constants of $^{3}J_{HH} = 2.5$ Hz indicates a trans disubstitution of the β-lactam ring (Fig. 5). Analogously, the substitution patterns on both β-lactam rings of all the bis-β-lactams **16a–f** have been assigned *trans*.

Although we depict only one structure for **16e** in which both β-lactam rings have *trans* stereochemistry, we cannot definitively determine the relative stereochemistry across the naphthalimide ring system as being *cis* or *trans* (or a mixture of both). In fact, two diastereomeric products **16e** having *trans* disubstitution on each of the β-lactam rings are possible (Fig. 6). From the ^{1}H NMR and ^{13}C NMR spectral data, however, only one set of resonances for each proton signal is observed, indicative of a single diastereomer.

Table 1 Structures and % yields of naphthalimido *cis*-β-lactams **11a-l**

Cpd	*β*-Lactam	Yield (%)	Cpd	*β*-Lactam	Yield (%)
11a	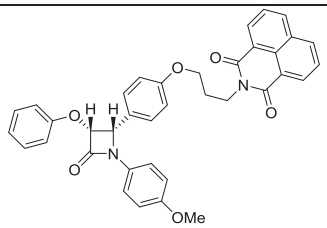	**90**	**11b**	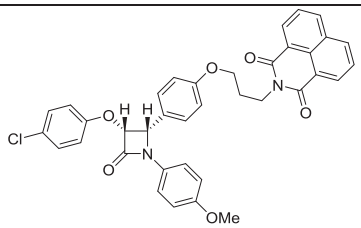	**85**
11c	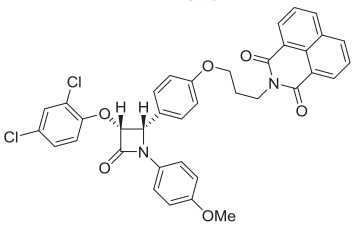	**85**	**11d**	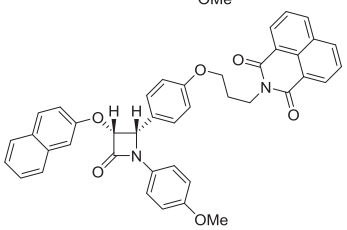	**78**
11e	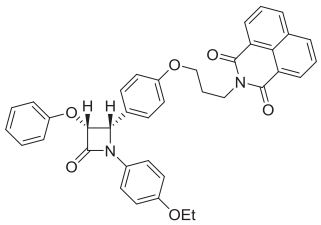	**95**	**11f**	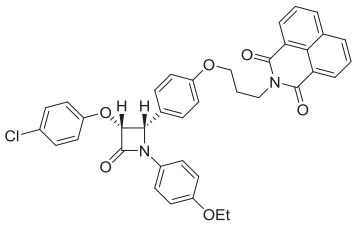	**90**
11g	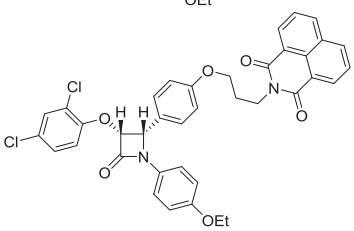	**90**	**11h**	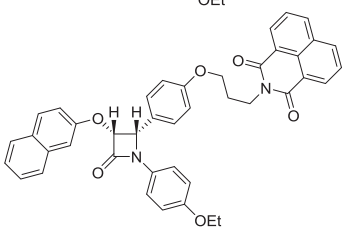	**75**
11i	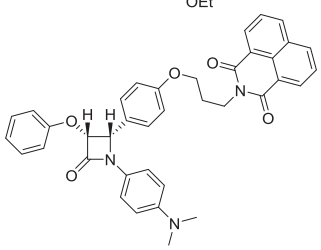	**90**	**11j**	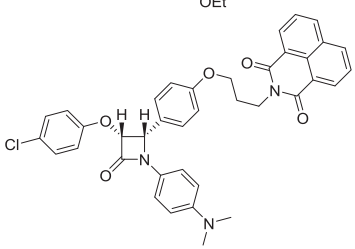	**82**
11k	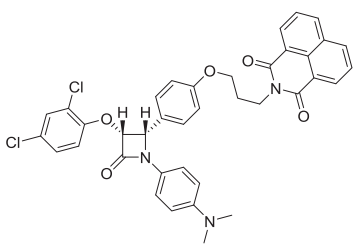	**80**	**11l**	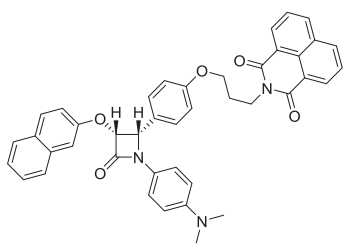	**75**

A plausible mechanism for the formation of the β-lactams is outlined in Scheme 3. The first step of the reaction involves a nucleophilic attack of the imino nitrogen on the ketene carbon to form zwitterionic intermediates **17** as a possible mixture of *cis* and *trans* species. These species may interconvert by way of the initial imine–ketene addition being reversible. The *cis* and *trans* β-lactam adducts result from subsequent ring closure of the zwitterionic species. The ratio of *cis–trans* cycloadducts depends on a variety of experimental factors, including the kinetics of the

final ring closure step, the rate of interconversion of the two zwitterions **17** as a function of temperature, electronic and steric nature of the substituents, and solvent (Cossio et al. 1993; Landa et al. 2018).

Typically, it is difficult to predict the stereochemical outcome a priori for new ketene–imine coupling partners, particularly those bearing large multicyclic aryl substituents, which can experience unexpectedly larger or smaller steric interactions due to skewed alignment of the rings in space, or conversely, steric bumping, as well as π–π interactions that can be either attractive (π-stacking) or electronically repulsive in their nature. Our experiments indicate that aryloxyacetic acids **10a–d** combine with the aryl imines **9** to afford only *cis*-β-lactams, while the bulky bis-arylimidoacetic acid **14** undergoes imine cycloaddition to yield only the *trans*-β-lactam products. The chemical shifts of the β-lactam ring protons of **16a–d** are near 7 ppm due to the deshielding effect of the anthracene ring, as evidenced in our previous publication (Borazjani et al. 2019a, 2019b).

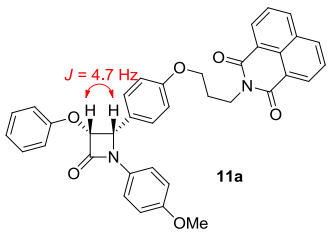

Fig. 3 Assignment of *cis*-stereochemistry for β-lactam **11a**

Antioxidant activity assay

The antioxidant capabilities of the mono and bis-β-lactam adducts, **11a–l** and **16a–g**, respectively, was evaluated using a diphenylpicrylhydrazyl (DPPH) radical-scavenging assay (Ayati et al. 2018; Kostova et al. 2011; Benzie and Strain 1999; Kamboj et al. 2019). Each compound was dissolved in DMSO and added to a solution of the DPPH in methanol, and the UV absorbance at 517 nm was measured. Percent radical-scavenging activity was determined mathematically from the absorbance after 5 min versus prior to the addition of the lactam. Among the compounds tested, bis-β-lactams **16a–d** showed excellent antioxidant activity with IC_{50} values of 15, 14.8, 7, 32.3 µg/ml, respectively, compared with the control standard (vitamin C) which had an IC_{50} value of 195 µg/ml. The other compounds showed much weaker free radical-scavenging activity with IC_{50} values between 4800 and 10,000 µg/ml. The preliminary structure-activity relationship (SAR) study of bis-β-lactam hybrids **16a–d** reveals that the presence of an anthracenyl moiety at the C-4 position of the β-lactam ring substantially increased antioxidant activity relative to a fluorenyl or 3,4-dimethoxyphenyl side group (Table 2).

Anticancer activity and cytotoxicity assays

HepG2, *MCF-7*, and *TC-1* cell lines were exposed to the various concentrations of the synthesized compounds for 24 h using MTT assay for estimation of cytotoxicity. The compounds **16a** and **16b** demonstrated excellent anticancer activity against the *MCF*-7 with IC50 values of 136.40,

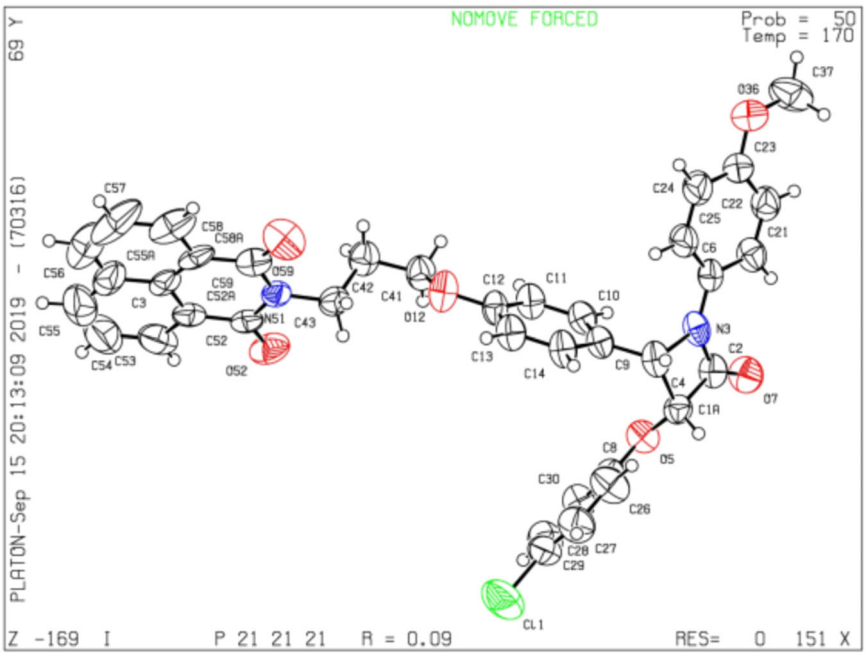

Fig. 4 ORTEP diagram of β-lactam **11b**

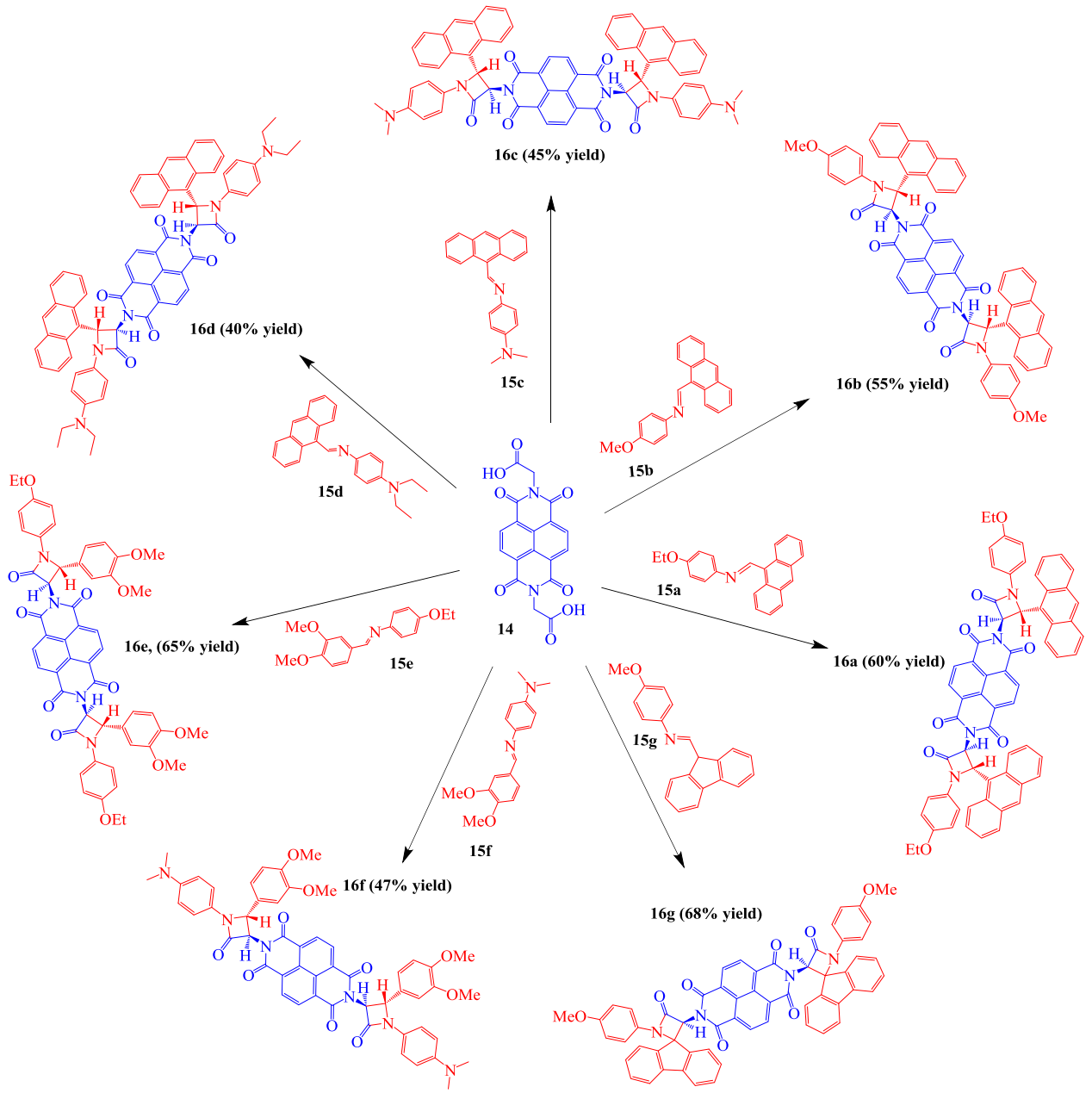

Scheme 2 Synthesis of bis-β-lactam adducts **16a–g**

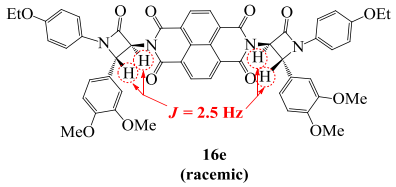

Fig. 5 Assignment of dual trans stereochemistry for bis-β-lactam **16e**

131.52 µM, respectively, in comparison to the anticancer agent Gemcitabin (IC_{50} of 191.57 µM) and raised up anticancer activity of **14**, **16a**, **16b**, **16c**, **16d**, **16e**, **16f**, and **16g** against the *TC-1* with IC_{50} values of 85.51, 69.55, 85.34, 89.37, 64.89, 189.16, 108.54, and 231.01 µM, respectively, in comparison to the anticancer agent Gemcitabine (IC_{50} of 153.25 µM) (Alami et al. 2007). The compounds **7** and **9c** showed good anticancer activity with IC_{50} values of 311.29 and 321.95 µM on TC-*1* cell lines. Also, good anticancer activity against the *MCF-7* with IC_{50} values of 400.01, 213.66, and 261.93 µM for compounds of **16c**, **16d,** and **16e**, respectively. Since all of these lactams

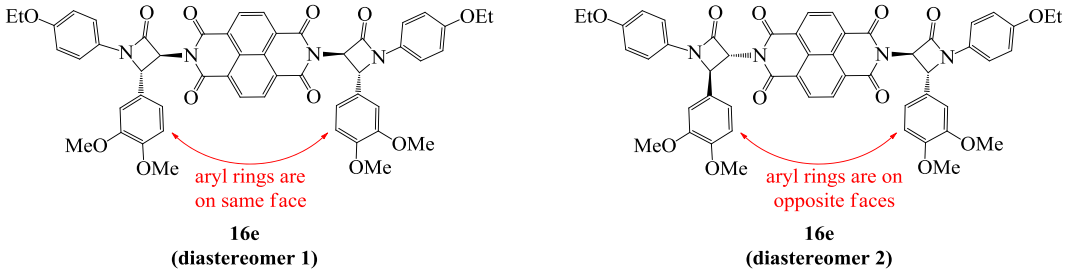

Fig. 6 Structures of the two possible bis-trans β-lactams **16e**

Scheme 3 A mechanism for discriminating between the *cis* versus *trans* stereochemistry of the β-lactams

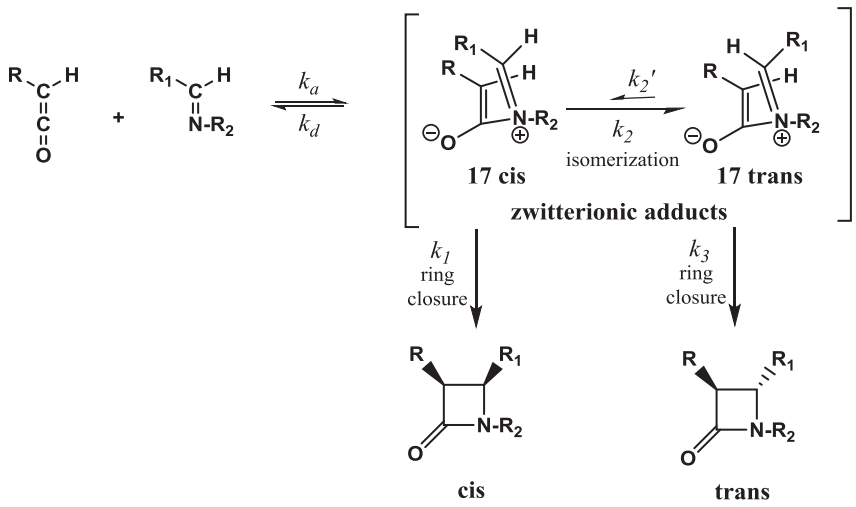

Table 2 Antioxidant activity of bis-lactams **16a–g** measured as IC_{50} scavenging of the DPPH radical

Compounds	IC_{50} (μg/ml)
16a	15
16b	14.8
16c	7
16d	32.3
16e	320
16f	445
16g	275
Vitamin C	195
DMSO blank	–

with excellent anticancer activity carry bis-naphthalimide on C-3 of the β-lactam ring, the aryl substituents at *N*-1 and C-4 of the β-lactam ring are responsible for these differences in activity. A tentative SAR exists, in that the presence of an anthracene moiety on C-4 of the *β*-lactam ring and a *p*-methoxyphenyl, *p*-ethoxyphenyl, *p*-*N*,*N*-dimethylaminophenyl or *p*-*N*,*N*-diethylaminophenyl ring on *N*-1 of the *β*-lactam provide the best anticancer bioactivity. On the other hand, there is no any cytotoxic effect on *HepG2* cell line based on tested concentrations (5, 10, 50, 100, and 200 μM) in comparison to high cytotoxicity of *HepG2* of Gemcitabine (IC_{50} of 215.01 μM) (Table 3). The possible mechanism for their anticancer activity might be related to production of intracellular free radicals, which ultimately led to cell apoptosis. Therefore, these compounds provide an opportunistic remedy for curing cancer diseases.

DNA interaction studies

UV/Vis titration assays

UV–visible absorption spectroscopy is an informative method to assess the binding interactions of compounds with DNA. Electronic absorption signal of compound undergoes changes when bound to DNA. Hyperchromicity or hypochromicity of the absorption signal can demonstrate the mode of interaction with DNA (Mondal et al. 2018). In this study, to get further insight into the naphthalimide derivatives-DNA interaction, we carry out a quantitative analysis of the binding process toward CT-DNA using **16a**, **16b**, **16d–g**, as model compounds. The absorption spectra of our compound in the presence of varying concentration of CT-DNA is shown in Fig. 7. Upon addition of calf-thymus DNA to **16a** and **16b**, there is an increase in molar absorptivity (hyperchromism) of the absorption bands at 362, 380, and 398 nm of both compounds. In its absorption

Table 3 Anticancer and cytotoxic activity assays assessed by the MTT reduction method against *MCF-7*, *TC-1*, and *HepG2* cell lines

Compounds	MCF-7 IC_{50} (μM)	TC-1 IC_{50} (μM)	HepG2 IC_{50} (μM)
7	>1000	311.29	>1000
9a	>1000	>1000	>1000
9b	>1000	>1000	>1000
9c	>1000	321.95	>1000
11a	>1000	>1000	>1000
11b	>1000	>1000	>1000
11c	>1000	>1000	>1000
11d	>1000	>1000	>1000
11e	>1000	>1000	>1000
11f	760.43	>1000	>1000
11g	508.96	>1000	>1000
11h	>1000	>1000	>1000
11i	>1000	>1000	>1000
11j	>1000	>1000	>1000
11k	>1000	>1000	>1000
11l	972.49	>1000	>1000
14	>1000	85.51	>1000
16a	136.40	69.55	>1000
16b	131.52	85.34	>1000
16c	400.01	89.37	>1000
16d	213.66	64.89	>1000
16e	261.93	189.16	>1000
16f	718.55	108.54	>1000
16g	760.69	231.01	>1000
Gemcitabine	191.57	153.25	215.01

spectra, **16e** exhibited two bands at 362 and 382 nm. Upon addition of CT-DNA, hyperchromism without any appreciable change in peak position was observed. Similarly, addition of CT-DNA to a solution of **16g** led to hyperchromic shift in the position of the transitions at 361 and 383 nm and bands did not show any significant shift. This type of behavior suggests a non-intercalative mode of interaction (Mondal et al. 2018; Kumar Gupta et al. 2013). Notably, **16d** and **16f** showed different behavior in CT-DNA titration studies. Addition of CT-DNA to a solution of **16d** led to a hypochromic shift of the band at 361 and 381 nm. **16f** exhibited similar behavior under the same conditions. Increase in the concentration of CT-DNA caused decrease in the absorbance intensity for the band at 362 and 382 nm of **16f** without any significant change in peak position. Conversely, the observed hypochromism in **16d** and **16f** suggested that these two compounds could insert into the base pairs of DNA and thus bind to CT-DNA by intercalation (Bhat et al. 2010). The DNA binding affinities of **16a**, **16b**, **16d–g** were compared quantitatively by calculating the intrinsic binding constant K_b using the Eq. (1):

$$[\mathrm{DNA}]/(\varepsilon_a - \varepsilon_f) = [\mathrm{DNA}]/(\varepsilon_b - \varepsilon_f) + 1/K_b(\varepsilon_b - \varepsilon_f) \quad (1)$$

where [DNA] stands for the concentration of DNA in base pairs, ε_a corresponds to the apparent extinction coefficient, ε_f is the extinction coefficient of the compound in its free form, and ε_b is the extinction coefficient of the compound in the bound form. When data fitted into the above equation, gave a straight line with the intercept of $1/K_b$ $(\varepsilon_b - \varepsilon_f)$ and slope of $1/(\varepsilon_b - \varepsilon_f)$ and the corresponding K_b value, are evaluated from the ratio of slope to intercept (Fig. 8 and Table 4). The observed K_b values indicating strong binding of these compounds with DNA and these are in the range for that of other naphthalimide derivatives compounds (Milelli et al. 2012). The binding affinity of our compounds thus vary in the order of **16a; 16b; 16e; 16g > 16d**; **16f**.

Fluorescence quenching studies

To further investigate the potential interactions of the bis-lactams **16a–g** with CT-DNA, a standard fluorescence quenching technique was carried out (Mandegani et al. 2016; Suh and Chaires 1995). Among these seven compounds, **16d** provided optimal fluorescence at room temperature in aqueous solution with an emission maxima at 520 nm after excitation at 420 nm. As shown in Fig. 9a, the emission intensities of compound **16d** decreased with increasing concentration of CT-DNA, and the wavelength showed a slight blue shift of 2 nm. The observed quenching is attributed to the strong binding of **16d** with CT-DNA, while the blue shift is consistent with intercalation (Banerjee et al. 2013; Li et al. 2014). The apparent DNA binding constant (K_b) for **16d** was determined from Eq. (2):

$$\log F_0 - F/F = log\, K_b + n \log[\mathrm{Q}] \quad (2)$$

where F_0 and F are the fluorescence intensity in the absence and the presence of the quencher **16d** at various concentrations, respectively, K_b is the binding constant, and n is the binding number. The K_b value was found to be 1.896×10^5 (Fig. 9b). These observations are in good agreement with the above absorption titration data and indicate that **16d** binds to DNA by intercalation.

Molecular docking studies

In order to confirm the biological results and to get insight into the interaction and binding mode of the most potent compound, molecular modeling studies were performed. The binding site and interactions of **16d** with DNA are illustrated in Fig. 10. DNA intercalation can often be seen

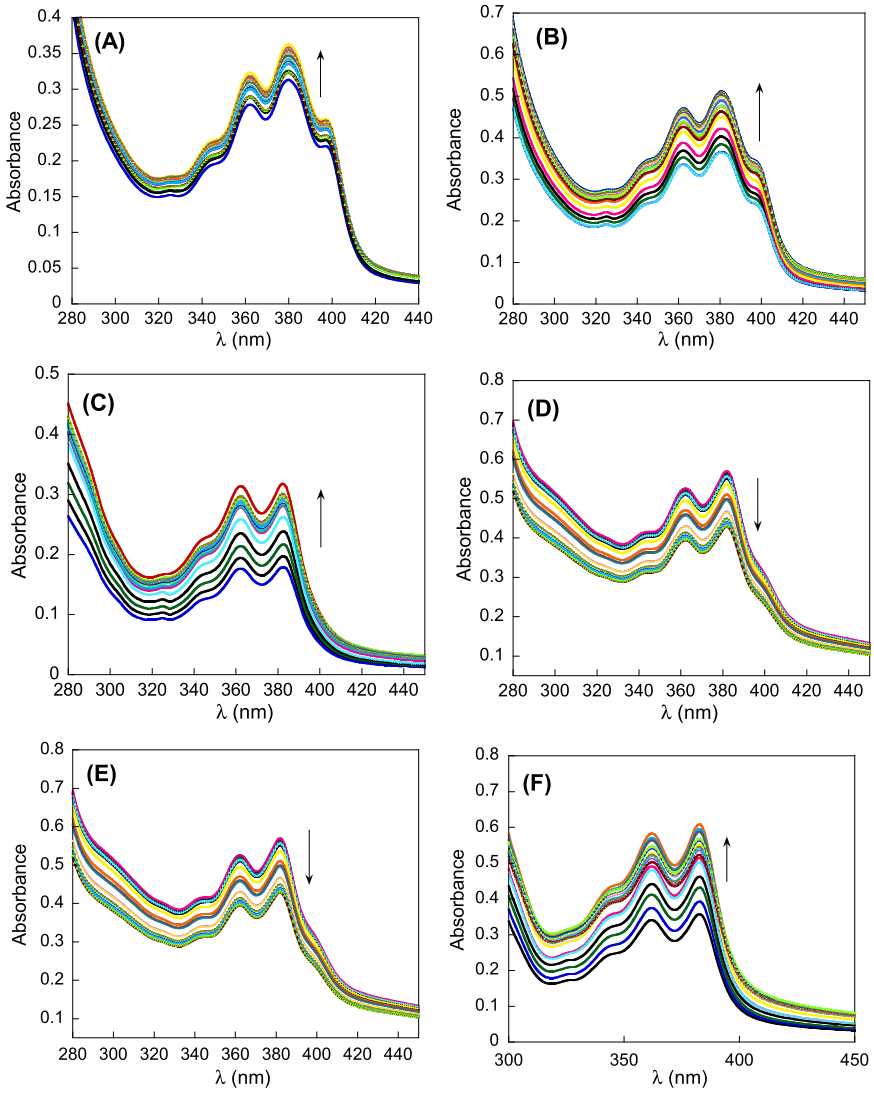

Fig. 7 Absorption titration spectra of **16a** (**a**), **16b** (**b**), **16e** (**c**), **16d** (**d**), **16f** (**e**), and **16g** (**f**) in 50 mM Tris-HCl buffer at pH 7.4, in the absence and presence of increasing amounts of DNA (0–7 μM in **16a**, 0–16 μM **16e**, 0–20 μM **16d**, **16f**, and 0–12 μM **16b**, **16g**)

for compounds having a planar polycyclic core (Zanoza et al. 2019; Arunadevi et al. 2019; Li et al. 2020; Arif et al. 2020). Unexpectedly, the anthracene motif of **16d** did not completely participate in intercalation between DNA base pairs; however, it oriented in a way that the diethylamine group could place within DC21 and DC22 base pairs and demonstrated hydrogen bond interaction between the nitrogen of diethylamine with the side chains of the DNA base pairs (DC22). Moreover, the methyl group of the diethylamine side chain also demonstrated π–σ interaction with a guanine of the DNA backbone. The benzene ring of diethylaniline also exhibited π–anion interactions with the phosphate backbone of DNA (DC21). The aromatic rings of the anthracene ring were observed to be involved in π–π stacking and π–lone pair interactions with the DT19 base pair and phosphate group, respectively. However, the other side of the molecule possesses the criteria for interaction with the minor grove, which is confirmed with molecular docking experiments. Bis-lactam **16d** perfectly orients in a curved shape along the length of the minor groove. The anthracene rings on the side chain were involved in three π–π stacking interactions with the DT8 base pair and π–lone pair interactions with the DNA phosphate groups. Moreover, the *N*,*N*-diethylaniline substituent was stabilized through a π–σ interaction with the DC9 DNA base pairs. Our results of molecular docking indicated that **16d** can potentially bind to the DNA groove and behave as a DNA intercalator, with the minimum binding energy of −10.18 kcal/mol. These data support the interaction of **16d** with DNA by intercalation.

The binding mode of Gemcitabine as a positive control with DNA (PDB code:453D, B-DNA [(5′-D(*CP*GP*CP*GP*AP*AP*TP*TP*CP*GP*CP*G)]) was defined by docking study to evaluate the mode of interaction with the target. As shown in Fig. 11, the interaction of

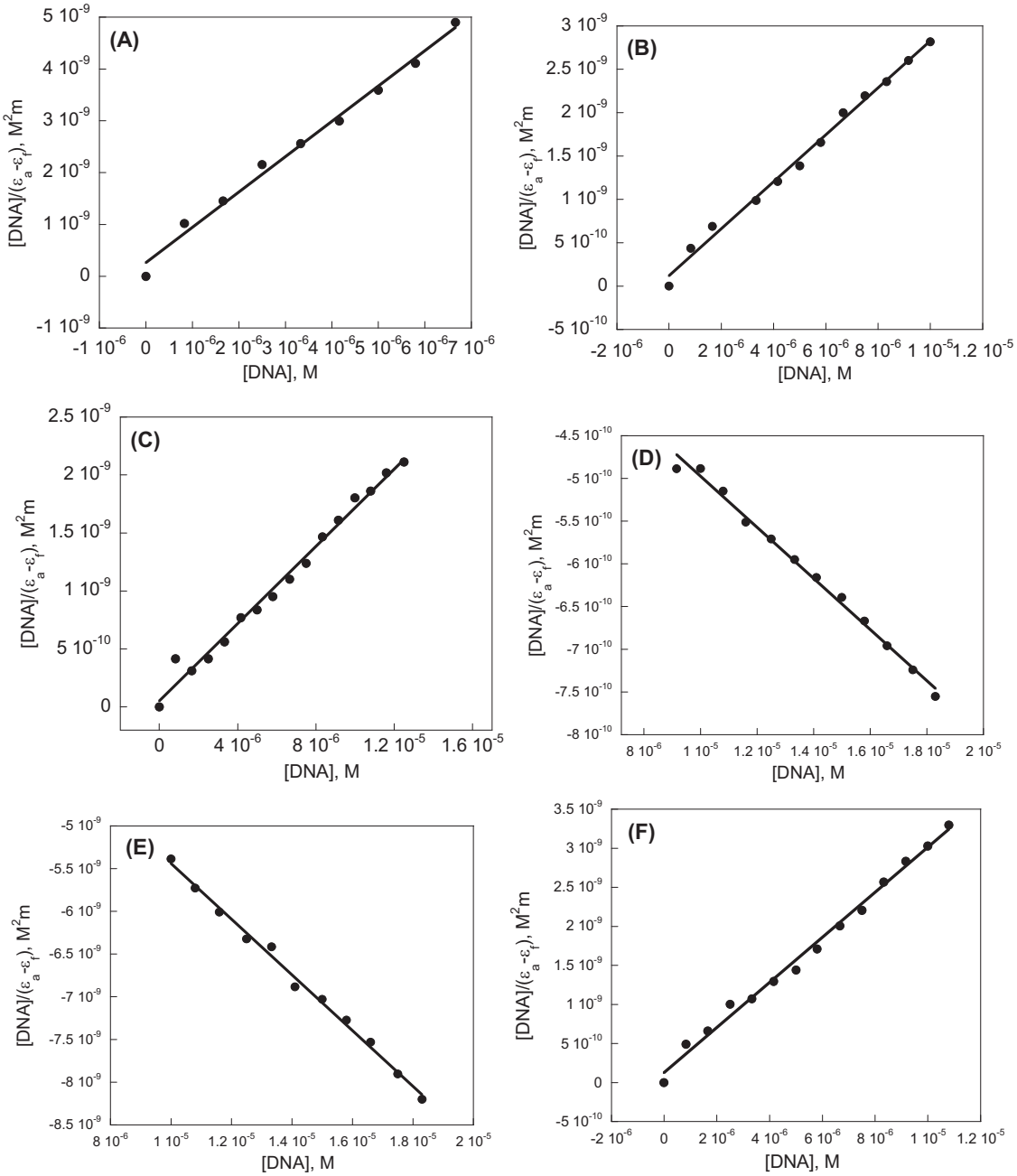

Fig. 8 Comparative plots of $[DNA]/(\varepsilon_a - \varepsilon_f)$ vs. [DNA] for **16a** (**a**), **16b** (**b**) **16e** (**c**), **16d** (**d**), **16f** (**e**), and **16g** (**f**)

this compound with nucleobases involved in hydrogen bond between the NH_2 group of Gemcitabine and thymine of DT7 base pair. Beside, NH of Gemcitabine also formed a hydrogen bond with base pair of DT20. It seems that aminopyrimidin-one fragment of Gemcitabine behaves like DNA-intercalating agents. Noteworthy, interaction with minor groove observed between hydroxymethyl group of Gemcitabine and DT10 of the DNA backbone. Another HB-interaction was observed between OH moiety of Gemcitabine and DT20 the backbone of DNA.

Conclusions

Although there are an assortment of methods for synthesizing functionalized β-lactam compounds, the Staudinger acid chloride-imine cycloaddition reaction is most widely used, because of both the simplicity in the methodology and the control of relative stereochemistry. In this study, we synthesized a selection of naphthalimido hybrids having one or two β-lactam side chains. Mono β-lactams **11a–l** are exclusively formed as *cis* stereoisomer, while both β-lactam

rings in the bis-β-lactams **16a–g** are *trans* disubstituted. Each of the β-lactams were evaluated for antioxidant activity. The best antioxidant activity was observed for compounds **16a–d** (15, 14.8, 7, 32.3 µg/mL, respectively). The bis-β-lactams **16a–g** display in vitro anticancer activity against the *MCF-7* and *TC-1* cancer cell lines, without noticeable cytotoxicity towards healthy cells. UV–vis and fluorescence spectroscopic studies have revealed the ability of our compounds to bind to CT-DNA. The activity of these compounds, based on their calculated DNA binding constant values, indicated that **16a**, **16b**, **16e**, **16g** > **16d**, **16f**. The obtained results are consistent with a DNA intercalation mechanism for both **16d** and **16f** and non-intercalation mechanism for **16a**; **16b**; **16e** and **16g**. These results of computational evaluations of **16d** is in agreement with the DNA binding studies as well as the cytotoxicity data. Molecular docking suggested two DNA binding modes for bis-naphthalimido β-lactam **16d**, that of minor roove and base pair intercalation.

Experimental section

General

Infrared analyses were done on a FT-IR 8300 spectrophotometer using potassium bromide pellets (υ in cm^{-1}). ^{1}H NMR and ^{13}C NMR spectra were recorded on a Bruker-Avance400 using a Bruker Avance DPX instrument (250 MHz, 400 MHz for ^{1}H NMR and 100 MHz for ^{13}C NMR). ^{13}C NMR spectral data were reported with complete proton decoupling. Chemical shifts were reported in parts per million (δ) downfield from tetramethylsilane. Splitting patterns are indicated as *s*: singlet, *d*: doublet, *t*: triplet, *q*: quartet, *m*: multiplet, *dd*: doublet of doublet. Coupling constants (*J*) are reported in hertz (Hz). Elemental analyses were run on a Thermo Finnigan Flash EA-1112 series. Thin-layer chromatography was carried out on silica gel 254. Melting points were recorded on a Buchi 510 melting point apparatus in open capillary tubes. The mass spectra were recorded on a Shimadzu GC-MS QP 1000 EX instrument. CH_2Cl_2 and Et_3N were dried before use by distillation over CaH_2.

Table 4 Binding constant of the interaction of **16a**, **16b**, **16d–g** with CT-DNA at 25 °C in 50 mM Tris-HCl buffer at pH 7.4

Compound	λ (nm)	K_b (M^{-1})	R^{2a}
16a	380	$2.575 \times 10^{+6}$	0.9906
16b	380	$2.279 \times 10^{+6}$	0.9936
16d	382	$1.552 \times 10^{+5}$	0.9906
16e	382	$2.567 \times 10^{+6}$	0.9936
16f	383	$1.578 \times 10^{+5}$	0.9934
16g	383	$2.329 \times 10^{+6}$	0.9923

R^{2a} is the linear correlated coefficient

General procedure for the synthesis of 4-(3-(1,3-dioxo-1*H*-benzo[*de*]isoquinolin-2(3*H*)-yl)propoxy) benzaldehyde (7)

1,8-Naphthalimide (**3**) was synthesized by the reaction of 1,8-naphthalic anhydride (**1**) (1.00 mmol) and ammonium acetate (**2**) (1.20 mmol) in DMF at 60 °C for an appropriate time. Then the crude was cooled to room temperature and recrystallized from ethanol to give compound **3**. Compound **3** (1.00 mmol), 1,3-dibromopropane (**4**) (3.00 mmol) and solid K_2CO_3 (3.00 mmol) in DMF was stirred at room temperature overnight. Water (10 mL) was added to the mixture and the precipitate was filtered and washed with petroleum ether. Compound **5** was recrystallized from ethanol [31]. A mixture of compound **5** (1.00 mmol), 4-hydroxybenzaldehyde (**6**) (1.20 mmol), solid K_2CO_3 (3.00 mmol) was stirred in acetonitrile at 70–80 °C for 24 h. After completion of the reaction, the crude was cooled to room temperature. The obtained precipitate was filtered and recrystallized from ethanol to give compound **7**.

4-(3-(1,3-Dioxo-1*H*-benzo[*de*]isoquinolin-2(3*H*)-yl)propoxy) benzaldehyde (7)

White solid; Mp. 188–200 °C; IR (KBr, cm^{-1}): 1699 (CO Naph), 1674 (CO Aldehyde), 1657 (CO Naph); ^{1}H NMR

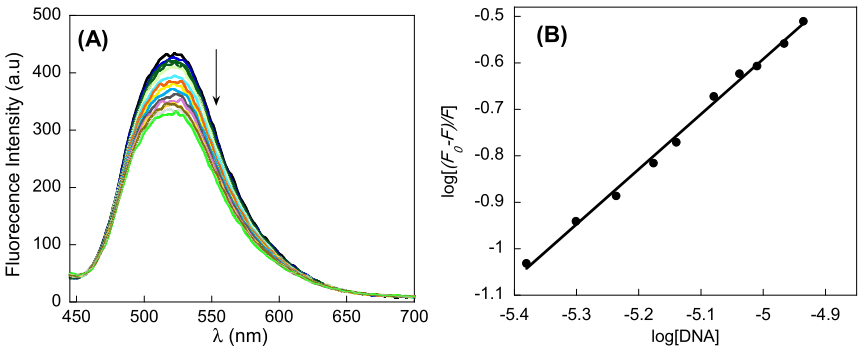

Fig. 9 **a** Fluorescence emission spectra of **16d** (20 µM) in the presence of increasing concentrations of CT-DNA (0–12 µM). The excitation wavelength was 420 nm. Spectra were recorded in the range of 440–820 nm in 50 mM Tris-HCl buffer at pH 7.4 in 100 mM aqueous NaCl. **b** Plot of log $[(F_0 - F)/F]$ versus log[DNA] at 25 °C

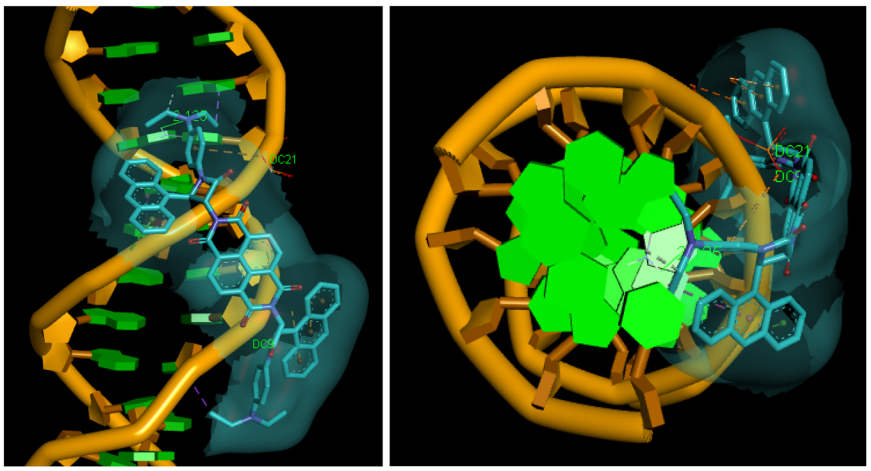

Fig. 10 Molecular modeling studies of bis-lactam **16d** with CT-DNA

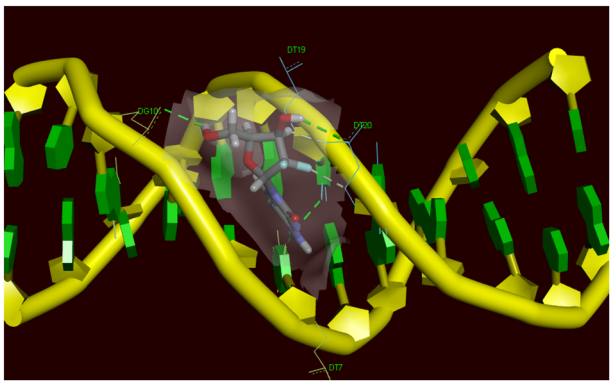

Fig. 11 Molecular modeling studies of Gemcitabine with CT-DNA

(250 MHz, DMSO-d_6): 2.09–2.19 (2H, m, –CH_2), 4.16–4.27 (4H, m, –NCH_2, –OCH_2), 6.97 (2H, *d*, *J* = 8.7 Hz, ArH), 7.78 (2H, *d*, *J* = 8.7 Hz, ArH), 7.85 (2H, *t*, *J* = 8.2 Hz, ArH), 8.43–8.48 (4H, m, ArH), 9.82 (1H, *s*, CHO); ^{13}C NMR (100 MHz, DMSO-d_6) δ 191.2 (CO Aldehyde), 163.4 (CO Naph), 134.2, 131.6, 131.2, 130.6, 129.4, 127.3, 127.1, 122.0, 114.7 (aromatic carbons), 66.4 (–OCH_2), 37.1 (–NCH_2), 27.2 (–CH_2); Analysis calculated for $C_{22}H_{17}NO_4$: C, 73.53; H, 4.77; N, 3.90%. Found: C, 73.12; H, 4.93; N, 3.43%.

General procedure for preparation of Schiff bases 9a–c

A mixture of compound **7** (1.00 mmol) and aniline derivatives **8a–c** (1.00 mmol) was refluxed in ethanol and 2–3 drops of AcOH for an appropriate time. Then the mixture was cooled to room temperature. The mixture of reaction was filtered and the solvent was evaporated under the reduced pressure. After that precipitate was recrystallized from ethanol to give Schiff bases **9a–c**.

2-(3-(4-(((4-Methoxyphenyl)imino)methyl)phenoxy)propyl)-1*H*-benzo[*de*]isoquinoline-1,3(2*H*)-dione (9a)

White solid; Mp. 172–174 °C; IR (KBr, cm^{-1}): 1696 (CO Naph), 1659 (CO Naph), 1624 (CH=N); ^{1}H NMR (250 MHz, DMSO-d_6): 2.08–2.18)2H, m, –CH_2), 3.75 (3H, *s*, OCH_3), 4.14 (2H, *t*, *J* = 6.0 Hz, –NCH_2), 4.24 (2H, *t*, *J* = 6.7 Hz, OCH_2), 6.88–6.95 (4H, *m*, ArH), 7.21 (2H, *d*, *J* = 7.7 Hz, ArH), 7.76 (2H, *d*, *J* = 8.2vHz, ArH), 7.85 (2H, *t*, *J* = 7.7 Hz, ArH), 8.43 (1H, *s*, CH=N), 8.46–8.48 (4H, *m*, ArH); ^{13}C NMR (100 MHz, DMSO-d_6) δ 163.5 (CO Naph), 160.8, 157.6, 157.5, 144.4, 134.2, 130.6, 130.0, 129.4, 129.0, 127.3, 127.1, 122.2, 122.1, 114.5, 114.3 (aromatic carbons and imine carbon), 66.1 (–OCH_2), 55.2 (OCH_3), 37.3 (–NCH_2), 27.3 (–CH_2); Analysis calculated for $C_{29}H_{24}N_2O_4$: C, 74.98; H, 5.21; N, 6.03%. Found: C, 74.58; H, 5.25; N, 6.15%.

2-(3-(4-(((4-Ethoxyphenyl)imino)methyl)phenoxy)propyl)-1*H*-benzo[*de*]isoquinoline-1,3(2*H*)-dione (9b)

Cream solid; Mp. 184–186 °C; IR (KBr, cm^{-1}): 1701 (CO Naph), 1663 (CO Naph), 1627 (CH=N); ^{1}H NMR (250 MHz, DMSO-d_6): 1.31 (3H, *t*, *J* = 7.0 Hz, CH_3), 2.09–2.18 (2H, m, –CH_2), 4.01 (2H, *q*, *J* = 7.0 Hz, OCH_2), 4.14 (2H, *t*, *J* = 5.7 Hz, –NCH_2), 4.25 (2H, *t*, *J* = 6.5 Hz, –OCH_2), 6.89 (2H, *d*, *J* = 4.2 Hz, ArH), 6.92 (2H, *d*, *J* = 4.2 Hz, ArH), 7.20 (2H, *d*, *J* = 8.7 Hz, ArH), 7.76 (2H, *d*, *J* = 8.5 Hz, ArH), 7.85 (2H, *t*, *J* = 7.5 Hz, ArH), 8.43 (1H, *s*, CH=N), 8.46–8.48 (4H, *m*, ArH); ^{13}C NMR (100 MHz, DMSO-d_6) δ 163.6 (CO Naph), 160.4, 157.6, 156.9, 147.5, 134.2, 133.9, 133.7, 131.7, 130.7, 129.9, 129.3, 127.1, 122.1, 114.9, 114.5 (aromatic carbons and imine carbon), 66.2 (–OCH_2), 63.1 (–OCH_2), 36.8 (–NCH_2), 27.0 (–CH_2), 14.4 (CH_3); Analysis calculated for $C_{30}H_{26}N_2O_4$: C, 75.30; H, 5.48; N, 5.85 %. Found: C, 75.11; H, 5.13; N, 5.35%.

2-(3-(4-(((4-(Dimethylamino)phenyl)imino)methyl)phenoxy) propyl)-1*H*-benzo[*de*]isoquinoline-1,3(2*H*)-dione (9c)

Yellow solid; Mp. 169–171 °C; IR (KBr, cm^{-1}): 1698 (CO Naph), 1661 (CO Naph), 1620 (CH=N); ^{1}H NMR (250 MHz, DMSO-d_6): 2.07–2.17 (2H, m, $–CH_2$), 2.88 (6H, *s*, NCH_3), 4.13 (2H, t, $J = 5.5$ Hz, $–NCH_2$), 4.24 (2H, *t*, $J = 6.2$ Hz, $–OCH_2$), 6.72 (2H, *d*, $J = 9.0$ Hz, ArH), 6.87 (2H, *d*, $J = 8.5$ Hz, ArH), 7.18 (2H, *d*, $J = 9.0$ Hz, ArH), 7.73 (2H, *d*, $J = 8.5$ Hz, ArH), 7.85 (2H, *t*, $J = 8.0$ Hz, ArH), 8.43 (1H, *s*, CH=N), 8.46–8.49 (4H, *d*, $J = 6.0$ Hz, ArH); ^{13}C NMR (100 MHz, DMSO-d_6) δ 163.5 (CO Naph), 160.4, 154.7, 149.0, 140.2, 134.2, 131.2, 130.6, 129.6, 129.5, 127.3, 127.1, 122.1, 122.0, 114.4, 112.6 (aromatic carbons and imine carbon), 66.1 ($–OCH_2$), 40.2 (NCH_3), 37.3 ($–NCH_2$), 27.3 ($–CH_2$); Analysis calculated for $C_{30}H_{27}N_3O_3$: C, 75.45; H, 5.70; N, 8.80%. Found: C, 75.64; H, 5.41; N, 8.15%.

General procedure for synthesis of new naphthalimido β-lactam conjugates 11a–l

A mixture of Schiff base **9a–c** (1.00 mmol), triethylamine (5.00 mmol), substituted acetic acid **10a–d** (1.50 mmol) and tosyl chloride (1.50 mmol) in dry CH_2Cl_2 (15 ml) was stirred overnight at room temperature. Then it was washed with 1 N aqueous HCl (20 ml), saturated $NaHCO_3$ (20 ml) and brine (20 ml). The organic layer was dried (anhydrous Na_2SO_4), filtered and the solvent was evaporated to give crude product **11a–l**. Conjugates **11a–l** were purified by recrystallization from ethyl acetate.

2-(3-(4-(1-(4-Methoxyphenyl)-4-oxo-3-phenoxyazetidin-2-yl)phenoxy)propyl)-1*H*-benzo[*de*]isoquinoline-1,3(2*H*)-dione (11a)

White solid; Mp 200–202 °C; IR (KBr, cm^{-1}): 1751 (CO β-lactam), 1697 (CO Naph), 1658 (CO Naph); ^{1}H NMR (250 MHz, DMSO-d_6): 1.97–2.08)2H, *m*, $–CH_2$), 3.67 (3H, *s*, OCH_3), 3.96 (2H, *t*, $J = 6.2$ Hz, $–NCH_2$), 4.16 (2H, *t*, $J = 6.7$ Hz, $–OCH_2$), 5.59 (1H, *d*, $J = 4.7$ Hz, H-4 β-lactam), 5.76 (1H, *d*, $J = 4.7$ Hz, H-3 β-lactam), 6.70 (2H, *d*, $J = 8.5$ HZ, ArH), 6.78 (2H, *d*, $J = 7.5$ Hz, ArH), 6.84–6.95 (3H, *m*, ArH), 7.14 (2H, *d*, $J = 7.5$ Hz, ArH), 7.19–7.23 (4H, *m*, ArH), 7.82 (2H, *t*, $J = 7.7$ Hz, ArH), 8.41–8.44 (4H, *m*, ArH); ^{13}C NMR (100 MHz, DMSO-d_6) δ 163.4 (CO β-lactam), 162.1 (CO Naph), 158.5, 156.4, 155.8, 137.7, 134.2, 130.6, 130.0, 129.3, 129.1128.0, 127.1, 125.4, 122.0, 120.0, 118.4, 115.0, 114.5, 114.4 (aromatic carbons), 80.4 (C-3 β-lactam), 66.7 (-OCH_2), 62.6 (C-4 β-lactam), 55.2 (OCH_3), 37.3 ($–NCH_2$), 27.3 ($–CH_2$); Analysis calculated for $C_{37}H_{30}N_2O_6$: C, 74.23; H, 5.05; N, 4.68%. Found: C, 74.11; H, 4.93; N, 4.25%.

2-(3-(4-(3-(4-Chlorophenoxy)-1-(4-methoxyphenyl)-4-oxoazetidin-2-yl)phenoxy)propyl)-1*H*-benzo[*de*] isoquinoline-1,3(2*H*)-dione (11b)

White solid; Mp. 207–209 °C; IR (KBr, cm^{-1}): 1745 (CO β-lactam), 1702 (CO Naph), 1656 (CO Naph); ^{1}H NMR (250 MHz, DMSO-d_6): 1.98–2.06 (2H, *m*, $–CH_2$), 3.67 (3H, *s*, OCH_3), 3.97 (2H, *t*, $J = 5.7$ Hz, $–NCH_2$), 4.17 (2H, *t*, $J = 7.2$ Hz, $–OCH_2$), 5.59 (1H, *d*, $J = 4.7$ Hz, H-4 β-lactam), 5.77 (1H, *d*, $J = 4.7$ Hz, H-3 β-lactam), 6.70 (2H, *d*, $J = 8.5$ Hz, ArH), 6.81 (2H, *d*, $J = 9.2$ Hz, ArH), 6.89 (2H, *d*, $J = 9.0$ Hz, ArH), 7.18–7.22 (6H, *m*, ArH), 7.82 (2H, *t*, $J = 8.2$ Hz, ArH), 8.41–8.45 (4H, *m*, ArH); ^{13}C NMR (100 MHz, DMSO-d_6) δ 163.4 (CO β-lactam), 161.7 (CO Naph), 158.4, 155.9, 155.2, 134.2, 131.2, 130.6, 129.9, 129.2, 129.0, 127.3, 127.1, 125.4, 124.5, 122.1, 118.4, 116.8, 114.5, 114.0 (aromatic carbons), 80.5 (C-3 β-lactam), 65.8 ($–OCH_2$), 60.2 (C-4 β-lactam), 55.2 (OCH_3), 37.2 ($–NCH_2$), 27.3 ($–CH_2$); Analysis calculated for $C_{37}H_{29}ClN_2O_6$: C, 70.20; H, 4.62; Cl, 5.60; N, 4.42%. Found: C, 70.08; H, 4.35; N, 4.04%.

2-(3-(4-(3-(2,4-Dichlorophenoxy)-1-(4-methoxyphenyl)-4-oxoazetidin-2-yl)phenoxy)propyl)-1*H*-benzo[*de*] isoquinoline-1,3(2*H*)-dione (11c)

White solid; Mp. 211–213 °C; IR (KBr, cm^{-1}): 1745 (CO β-lactam), 1701 (CO Naph), 1656 (CO Naph); ^{1}H NMR (250 MHz, DMSO-d_6): 1.98–2.08 (2H, *m*, $–CH_2$), 3.67 (3H, *s*, OCH_3), 3.97 (2H, *t*, $J = 6.0$ Hz, $–NCH_2$), 4.16 (2H, *t*, $J = 6.7$ Hz, $–OCH_2$), 5.61 (1H, *d*, $J = 4.5$ Hz, H-4 β-lactam), 5.89 (1H, *d*, $J = 4.5$ Hz, H-3 β-lactam), 6.66 (2H, *d*, $J = 8.5$ Hz, ArH), 6.89 (1H, *d*, $J = 9.0$ Hz, ArH), 7.13 (1H, *d*, $J = 9.0$ Hz, ArH), 7.19–7.22 (4H, *m*, ArH), 7.27 (2H, dd, $J_1 = 9.0$ Hz, $J_1 = 2.5$ Hz, ArH), 7.38 (1H, *d*, $J = 2.5$ Hz, ArH), 7.82 (2H, *t*, $J = 8.0$ Hz, ArH), 8.41–8.44 (4H, *m* ArH); ^{13}C NMR (100 MHz, DMSO-d_6) δ 163.4 (CO β-lactam), 161.2 (CO Naph), 158.5, 155.9, 150.7, 134.2, 131.2, 130.6, 129.8, 129.3, 128.3, 127.7, 127.3, 127.1, 125.6, 124.6, 124.1, 122.1, 118.5, 116.0, 114.5, 114.1 (aromatic carbons), 80.6 (C-3 β-lactam), 65.8 ($–OCH_2$), 60.0 (C-4 β-lactam), 55.2 (OCH_3), 37.2 ($–NCH_2$), 27.3 ($–CH_2$); Analysis calculated for $C_{37}H_{28}Cl_2N_2O_6$: C, 66.57; H, 4.23; N, 4.20%. Found: C, 66.29; H, 4.08; N, 4.06%.

2-(3-(4-(1-(4-Methoxyphenyl)-3-(naphthalen-2-yloxy)-4-oxoazetidin-2-yl)phenoxy)propyl)-1*H*-benzo[*de*] isoquinoline-1,3(2*H*)-dione (11d)

White solid; Mp. 199–201 °C; IR (KBr, cm^{-1}): 1743 (CO β-lactam), 1702 (CO Naph), 1657 (CO Naph); ^{1}H NMR (250 MHz, DMSO-d_6): 1.93–2.04 (2H, *m*, $–CH_2$), 3.68 (3H,

s, OCH_3), 3.92 (2H, *t*, $J = 6.0$ Hz, $–NCH_2$), 4.13 (2H, *t*, $J = 7.0$ Hz, $–OCH_2$), 5.70 (1H, *d*, $J = 4.7$ Hz, H-4 β-lactam), 5.91 (1H, *d*, $J = 4.7$ Hz, H-3 β-lactam), 6.66 (2H, *d*, $J = 8.7$ Hz, ArH), 6.89–6.98 (3H, *m*, ArH), 7.21–7.34 (6H, *m*, ArH), 7.43 (1H, *t*, $J = 8.0$ Hz, ArH), 7.69 (1H, *d*, $J = 9.0$ Hz, ArH), 7.75 (2H, *d*, $J = 8.7$ Hz, ArH), 7.81 (2H, *d*, $J = 7.7$ Hz, ArH), 8.40–8.43 (4H, *m*, ArH); ^{13}C NMR (100 MHz, DMSO-d_6) δ 163.4 (CO β-lactam), 162.0 (CO Naph), 158.3, 155.9, 154.2, 134.1, 133.6, 131.2, 130.6, 130.0, 129.2, 128.8, 127.4, 127.3, 127.1, 126.7, 126.4, 124.7, 124.0, 122.0, 118.4, 117.8, 114.5, 114.0, 108.6 (aromatic carbons), 80.5 (C-3 β-lactam), 65.7 ($–OCH_2$), 60.4 (C-4 β-lactam), 55.2 (OCH_3), 37.2 ($–NCH_2$), 27.3 ($–CH_2$); Analysis calculated for $C_{41}H_{32}N_2O_6$: C, 75.91; H, 4.97; N, 4.32 %. Found: C, 75.77; H, 4.83; N, 4.28%.

2-(3-(4-(1-(4-Ethoxyphenyl)-4-oxo-3-phenoxyazetidin-2-yl) phenoxy)propyl)-1*H*-benzo[*de*]isoquinoline-1,3(2*H*)-dione (11e)

White solid; Mp. 198–200 °C; IR (KBr, cm^{-1}): 1750 (CO β-lactam), 1705 (CO Naph), 1656 (CO Naph); ^{1}H NMR (250 MHz, DMSO-d_6): 1.25 (3H, *t*, $J = 7.0$ Hz, CH_3), 1.96–2.07 (2H, *m*, $–CH_2$), 3.88–3.98 (4H, *m*, $–NCH_2$, $–OCH_2$), 4.16 (2H, *t*, $J = 6.5$ Hz, $–OCH_2$), 5.58 (1H, *d*, $J = 4.7$ Hz, H-4 β-lactam), 5.75 (1H, *d*, $J = 4.7$ Hz, H-3 β-lactam), 6.70 (2H, *d*, $J = 8.5$ Hz, ArH), 6.78 (2H, *d*, $J = 8.0$ Hz, ArH), 6.85–6.89 (3H, *m*, ArH), 7.13–7.23 (6H, *m*, ArH), 7.82 (2H, *t*, $J = 7.2$ Hz, ArH), 8.41–8.44 (4H, *m*, ArH); ^{13}C NMR (100 MHz, DMSO-d_6) δ 163.4 (CO β-lactam), 162.1 (CO Naph), 158.4, 156.5, 155.1, 134.2, 131.2, 130.6, 129.9, 129.3, 127.3, 127.1, 124.8, 122.0, 121.7, 118.4, 115.0, 114.9, 114.0 (aromatic carbons), 80.5 (C-3 β-lactam), 65.7 ($–OCH_2$), 63.1 ($–OCH_2$), 60.4 (C-4 β-lactam), 37.2 ($–NCH_2$), 27.3 ($–CH_2$), 14.5 (CH_3); Analysis calculated for $C_{38}H_{32}N_2O_6$: C, 74.50; H, 5.26; N, 4.57%. Found: C, 74.38; H, 5.05; N, 4.18%.

2-(3-(4-(3-(4-Chlorophenoxy)-1-(4-ethoxyphenyl)-4-oxoazetidin-2-yl)phenoxy)propyl)-1*H*-benzo[*de*] isoquinoline-1,3(2*H*)-dione (11f)

White solid; Mp. 203–205 °C; IR (KBr, cm^{-1}): 1758 (CO β-lactam), 1662 (CO Naph); ^{1}H NMR (250 MHz, DMSO-d_6): 1.25)3H, *t*, $J = 7.0$ Hz, CH_3), 1.99–2.08 (2H, *m*, $–CH_2$), 3.88–3.99 (4H, *m*, $–NCH_2$, $–OCH_2$), 4.17 (2H, *t*, $J = 6.7$ Hz, $–OCH_2$), 5.57 (1H, *d*, $J = 4.5$ Hz, H-4 β-lactam), 5.76 (1H, *d*, $J = 4.5$ Hz, H-3 β-lactam), 6.70 (2H, *d*, $J = 8.0$ Hz, ArH), 6.81 (2H, *d*, $J = 7.7$ Hz, ArH), 6.87 (2H, *d*, $J = 8.0$ Hz, ArH), 7.18–7.21 (6H, *m*, ArH), 7.82 (2H, *t*, $J = 8.0$ Hz, ArH), 8.41–8.44 (4H, *m*, ArH); ^{13}C NMR (100 MHz, DMSO-d_6) δ 163.4 (CO β-lactam), 161.7 (CO Naph), 158.4, 155.2, 154.8, 134.2, 131.2, 130.6, 129.8, 129.2, 129.0, 127.3, 127.1, 125.4, 124.5, 122.1, 118.4, 116.8, 114.9, 114.0 (aromatic carbons), 80.5 (C-3 β-lactam), 65.7 ($–OCH_2$), 63.1 ($–OCH_2$), 60.2 (C-4 β-lactam), 37.2 ($–NCH_2$), 27.3 ($–CH_2$), 14.5 (CH_3); Analysis calculated for $C_{38}H_{31}ClN_2O_6$: C, 70.53; H, 4.83; N, 4.33%. Found: C, 70.48; H, 4.23; N, 4.20%.

2-(3-(4-(3-(2,4-Dichlorophenoxy)-1-(4-ethoxyphenyl)-4-oxoazetidin-2-yl)phenoxy)propyl)-1*H*-benzo[*de*] isoquinoline-1,3(2*H*)-dione (11g)

White solid; Mp. 213–215 °C; IR (KBr, cm^{-1}): 1755 (CO β-lactam), 1701 (CO Naph), 1666 (CO Naph); ^{1}H NMR (250 MHz, DMSO-d_6): 1.25)3H, *t*, $J = 7.0$ Hz, CH_3), 2.00–2.06 (2H, m, $–CH_2$), 3.88–3.99 (4H, *m*, $–NCH_2$, $–OCH_2$), 4.16 (2H, *t*, $J = 6.7$ Hz, $–OCH_2$), 5.60 (1H, *d*, $J = 4.5$ Hz, H-4 β-lactam), 5.87 (1H, *d*, $J = 4.5$ Hz, H-3 β-lactam), 6.80 (2H, *d*, $J = 8.5$ Hz, ArH), 6.87 (2H, *d*, $J = 9.0$ Hz, H-3), 7.12 (1H, *d*, $J = 9.0$, ArH), 7.17–7.22 (4H, *m*, ArH) 7.27 (1H, dd, $J_1 = 10.7$ Hz, $J_2 = 2.5$ Hz, ArH), 7.37 (1H, *d*, $J = 2.5$ Hz, ArH), 7.81 (2H, *t*, $J = 7.7$ Hz ArH), 8.40–8.44 (4H, *m*, ArH); ^{13}C NMR (100 MHz, DMSO-d_6) δ 163.4 (CO β-lactam), 161.2 (CO Naph), 158.5, 155.2, 150.7, 134.2, 131.2, 130.6, 129.7, 129.3, 129.2, 127.7, 127.3, 127.1, 125.6, 124.1, 122.1, 122.0, 118.5, 116.0, 114.9, 114.1 (aromatic carbons), 80.6 (C-3 β-lactam), 65.8 ($–OCH_2$), 63.1 ($–OCH_2$), 60.0 (C-4 β-lactam), 37.2 ($–NCH_2$), 27.3 ($–CH_2$), 14.5 (CH_3); Analysis calculated for $C_{38}H_{30}Cl_2N_2O_6$: C, 66.97; H, 4.44; N, 4.11%. Found: C, 66.88; H, 3.93; N, 4.00%.

2-(3-(4-(1-(4-Ethoxyphenyl)-3-(naphthalen-2-yloxy)-4-oxoazetidin-2-yl)phenoxy)propyl)-1*H*-benzo[*de*] isoquinoline-1,3(2*H*)-dione (11h)

Cream solid; Mp. 182–184 °C; IR (KBr, cm^{-1}): 1738 (CO β-lactam), 1702 (CO Naph), 1662 (CO Naph); ^{1}H NMR (250 MHz, DMSO-d_6): 1.25)3H, *t*, $J = 6.7$ Hz, CH_3), 1.96–2.01 (2H, *m*, $–CH_2$), 3.86–3.97 (4H, *m*, $–NCH_2$, $–OCH_2$), 4.13 (2H, *t*, $J = 7.0$ Hz, $–OCH_2$), 5.69 (1H, *d*, $J = 4.2$ Hz, H-4 β-lactam), 5.91 (1H, *d*, $J = 4.2$ Hz, H-3 β-lactam), 6.66 (2H, *d*, $J = 5.7$ Hz, ArH), 6.88 (2H, *d*, $J = 8.7$ Hz, ArH), 6.95 (1H, *d*, $J = 9.7$ Hz, ArH), 7.23–7.30 (5H, *m*, ArH) 7.32 (1H, *t*, $J = 7.7$ Hz, ArH), 7.43 (1H, *t*, $J = 7.7$ Hz, ArH), 7.68 (1H, *t*, $J = 9.2$ Hz, ArH), 7.74 (2H, *d*, $J = 8.5$ Hz, ArH), 7.81 (2H, *d*, $J = 7.7$ Hz, ArH), 8.39–8.42 (4H, *m*, ArH); ^{13}C NMR (100 MHz, DMSO-d_6) δ 163.4 (CO β-lactam), 162.0 (CO Naph), 158.3, 155.1, 154.2, 134.1, 133.6, 131.1, 130.5, 129.9, 129.2, 128.8, 127.4, 127.3, 127.0, 126.7126.5, 124.7, 124.0, 122.0, 118.4, 117.8, 114.9, 114.0, 108.6 (aromatic carbons), 80.4 (C-3 β-lactam), 65.7 ($–OCH_2$), 63.1 ($–OCH_2$), 60.5 (C-4 β-lactam), 37.2 ($–NCH_2$), 27.3 ($–CH_2$), 14.5 (CH_3);

Analysis calculated for $C_{42}H_{34}N_2O_6$: C, 76.12; H, 5.17; N, 4.23%. Found: C, 76.08; H, 4.98; N, 4.12%.

2-(3-(4-(1-(4-(Dimethylamino)phenyl)-4-oxo-3-phenoxyazetidin-2-yl)phenoxy)propyl)-1*H*-benzo[*de*]isoquinoline-1,3(2*H*)-dione (11i)

Cream solid; Mp. 221–223 °C; IR (KBr, cm^{-1}): 1737 (CO β-lactam), 1703 (CO Naph), 1659 (CO Naph); ^{1}H NMR (250 MHz, DMSO-d_6): 1.96–2.07 (2H, m, –CH_2), 2.79 (6H, *s*, NCH_3), 3.95 (2H, *t*, $J = 6.0$ Hz, –NCH_2), 4.16 (2H, *t*, $J = 7.0$ Hz, –OCH_2), 5.54 (1H, *d*, $J = 4.7$ Hz, H-4 β-lactam), 5.71 (1H, *d*, $J = 4.7$ Hz, H-3 β-lactam), 6.64 (2H, *d*, $J = 9.0$ Hz, ArH), 6.69 (2H, *d*, $J = 8.5$ Hz, ArH), 6.75 (2H, *d*, $J = 7.7$ Hz, ArH), 6.83 (1H, *t*, $J = 7.2$ Hz, ArH), 7.09–7.13 (3H, *m*, ArH), 7.16–7.21 (3H, *m*, ArH), 7.81 (2H, *t*, $J = 8.2$ Hz, ArH), 8.40–8.43(4H, *m*, ArH); ^{13}C NMR (100 MHz, DMSO-d_6) δ 163.4 (CO β-lactam), 161.6 (CO Naph), 158.3, 156.5, 147.4, 134.1, 131.1, 130.5, 129.2, 127.3, 127.0, 126.5, 125.0, 122.0, 121.6, 118.3, 115.0, 113.9, 112.7 (aromatic carbons), 80.4 (C-3 β-lactam), 65.7 (-OCH_2), 60.3 (C-4 β-lactam), 40.1 (NCH_3), 37.2 (–NCH_2), 27.3 (–CH_2); Analysis calculated for $C_{38}H_{33}N_3O_5$: C, 74.61; H, 5.44; N, 6.87%. Found: C, 74.48; H, 5.38; N, 6.65%.

2-(3-(4-(3-(4-Chlorophenoxy)-1-(4-(dimethylamino)phenyl)-4-oxoazetidin-2-yl)phenoxy)propyl)-1*H*-benzo[*de*]isoquinoline-1,3(2*H*)-dione (11j)

Cream solid; Mp. 215–217 °C; IR (KBr, cm^{-1}): 1734 (CO β-lactam), 1705 (CO Naph), 1658 (CO Naph); ^{1}H NMR (250 MHz, DMSO-d_6): 1.97–2.07 (2H, m, –CH_2), 2.79 (6H, *s*, NCH_3), 3.96 (2H, *t*, $J = 5.5$ Hz, –NCH_2), 4.17 (2H, *t*, $J = 6.5$ Hz, –OCH_2), 5.53 (1H, *d*, $J = 4.5$ Hz, H-4 β-lactam), 5.73 (1H, *d*, $J = 4.5$ Hz, H-3 β-lactam), 6.64 (2H, *d*, $J = 9.0$ Hz, ArH), 6.69 (2H, *d*, $J = 10.0$ Hz, ArH), 6.81 (2H, *d*, $J = 9.0$ Hz, ArH), 7.10 (2H, *d*, $J = 9.0$ Hz, ArH), 7.16–7.21 (4H, *m*, ArH), 7.82 (2H, *t*, $J = 8.2$ Hz, ArH), 8.41–8.45 (4H, *m*, ArH); ^{13}C NMR (100 MHz, DMSO-d_6) δ 163.9 (CO β-lactam), 161.7 (CO Naph), 158.9, 155.7, 148.0, 134.7, 131.7, 131.1, 129.7, 129.5, 127.8, 127.6, 126.9, 125.8, 125.3, 122.6, 118.8, 117.3, 114.5, 113.2 (aromatic carbons), 80.9 (C-3 β-lactam), 66.3 (–OCH_2), 60.6 (C-4 β-lactam), 40.6 (NCH_3), 37.7 (–NCH_2), 27.8 (–CH_2); Analysis calculated for $C_{38}H_{32}ClN_3O_5$: C, 70.64; H, 4.99; N, 6.50%. Found: C, 70.56; H, 4.87; N, 6.42%.

2-(3-(4-(3-(2,4-Dichlorophenoxy)-1-(4-(dimethylamino)phenyl)-4-oxoazetidin-2-yl)phenoxy)propyl)-1*H*-benzo[*de*]isoquinoline-1,3(2*H*)-dione (11k)

Brown solid; Mp. 222–224 °C; IR (KBr, cm^{-1}): 1739 (CO β-lactam), 1702 (CO Naph), 1664 (CO Naph); ^{1}H NMR (250 MHz, DMSO-d_6): 2.00–2.09 (2H, *m*, –CH_2), 2.82 (6H, *s*, NCH_3), 3.99 (2H, *t*, $J = 5.5$ Hz, –NCH_2), 4.18 (2H, *t*, $J = 7.0$ Hz, –OCH_2), 5.59 (1H, *d*, $J = 4.5$ Hz, H-4 β-lactam), 5.87 (1H, *d*, $J = 4.5$ Hz, H-3 β-lactam), 6.67 (2H, *d*, $J = 9.0$ Hz, ArH), 6.72 (2H, *d*, $J = 8.7$ Hz, ArH), 7.12 (2H, *d*, $J = 3.7$ Hz, ArH), 7.16 (2H, *d*, $J = 3.7$ Hz, ArH), 7.22 (2H, *d*, $J = 8.5$ Hz, ArH), 7.29 (1H, dd, $J_1 = 11.0$ Hz, $J_2 = 2.5$ Hz, ArH), 7.40 (1H, *d*, $J = 2.5$ Hz, ArH), 7.83 (2H, *t*, $J = 7.7$ Hz, ArH), 8.42–8.46 (3H, *m*, ArH); ^{13}C NMR (100 MHz, DMSO-d_6) δ 163.4 (CO β-lactam), 160.6 (CO Naph), 158.4, 150.8, 147.5, 134.1, 131.1, 130.6, 129.2, 127.6, 127.3, 127.0, 126.3, 125.5, 124.5, 124.4, 122.1, 122.0, 118.3, 116.0, 114.0, 112.6 (aromatic carbons), 80.5 (C-3 β-lactam), 65.8 (-OCH_2), 59.9 (C-4 β-lactam), 40.1 (NCH_3), 37.2 (–NCH_2), 27.3 (–CH_2); Analysis calculated for $C_{38}H_{31}Cl_2N_3O_5$: C, 67.06; H, 4.59; N, 6.17%. Found: C, 66.92.; H, 4.44; N, 5.98%.

2-(3-(4-(1-(4-(Dimethylamino)phenyl)-3-(naphthalen-2-yloxy)-4-oxoazetidin-2-yl)phenoxy)propyl)-1*H*-benzo[*de*]isoquinoline-1,3(2*H*)-dione (11l)

Brown solid; Mp. 192–194 °C; IR (KBr, cm^{-1}): 1736 (CO β-lactam), 1702 (CO Naph), 1662 (CO Naph); ^{1}H NMR (250 MHz, DMSO-d_6): 1.93–2.00 (2H, *m*, –CH_2), 2.80 (6H, *s*, NCH_3), 3.90 (2H, *t*, $J = 5.7$ Hz, –NCH_2), 4.12 (2H, *t*, $J = 7.0$ Hz, –OCH_2), 5.65 (1H, d, $J = 4.7$ Hz, H-4 β-lactam), 5.87 (1H, *d*, $J = 4.7$ Hz, H-3 β-lactam), 6.63–6.68 (4H, *m*, ArH), 6.95 (1H, dd, $J_1 = 8.7$ Hz, $J_2 = 2.5$ Hz, ArH), 7.13 (2H, *d*, $J = 9.0$ Hz, ArH), 7.22–7.33 (5H, *m*, ArH), 7.42 (1H, *t*, $J = 8.0$ Hz, ArH), 7.67 (1H, *d*, $J = 9.2$ Hz, ArH), 7.72–7.81 (4H, *m*, ArH), 8.38–8.41 (3H, *m*, ArH); ^{13}C NMR (100 MHz, DMSO-d_6) δ 168.1 (CO β-lactam), 166.2 (CO Naph), 163.0, 159.0, 152.2, 150.6, 138.9, 138.4, 135.9, 135.3, 134.0, 133.5, 132.2, 132.0, 131.8, 131.4, 131.3, 131.2, 129.7, 128.7, 126.8, 123.0, 122.6, 118.7, 117.5, 113.3 (aromatic carbons), 85.1 (C-3 β-lactam), 70.4 (–OCH_2), 65.1 (C-4 β-lactam), 44.9 (NCH_3), 42.0 (–NCH_2), 32.0 (–CH_2); Analysis calculated for $C_{42}H_{35}N_3O_5$: C, 76.23; H, 5.33; N, 6.35%. Found: C, 76.08; H, 5.05; N, 6.12%.

General procedure for the synthesis of diacetic acid (14)

A mixture of 1,4,5,8-naphthalenetetracarboxylic dianhydride (**12**) (1.00 mmol) and glycine (2.20 mmol) was added in DMF (5 ml) and the mixture was stirred at 60 °C for several hours (TLC control in a solvent system *n*-hexane: ethyl acetate = 2:1). After cooling to room temperature 20 mL water was added to the mixture and the solid diacetic acid **14** was separated, the product was purified by recrystallization from ethanol and used for the next step.

2,2′-(1,3,6,8-Tetraoxo-1,3,6,8-tetrahydrobenzo[*lmn*][3,8] phenanthroline-2,7-diyl)diacetic acid (14)

Pink solid; Mp. 220–222 °C; IR (KBr, cm^{-1}): 2368–3400 (OH, acid), 1720 (CO acid and CO Naph), 1666 (CO Naph); ^{1}H NMR (400 MHz, DMSO-d_6) δ 4.77 (4H, *s*, $2CH_2$), 8.66 (4H, *s*, ArH), 13.34 (2H, brs, 2OH); ^{13}C NMR (100 MHz, DMSO-d_6) δ 169.4 (CO acid), 162.5 (CO Naph), 131.4, 126.6, 126.2 (aromatic carbons), 41.9 (CH_2); Analysis calculated for $C_{18}H_{10}N_2O_8$: C, 56.55; H, 2.64; N, 7.33%. Found: C, 56.40; H, 2.55; N, 7.27%.

General procedure for the bis-β-lactams 16a–g preparation (Staudinger reaction)

The appropriate aromatic imines (Schiff bases) (2.00 mmol), triethylamine (5.00 mmol), 1: 2,2′-(1,3,6,8-tetraoxo-1,3,6,8-tetrahydrobenzo[*lmn*][3,8]phenanthroline-2,7-diyl)diacetic acid (**14**) (1 mmol) and tosyl chloride (1.50 mmol) were added to anhydrous CH_2Cl_2 (5 mL) and the mixture was stirred at room temperature for 24 h (TLC control in a solvent system *n*-hexane: ethyl acetate = 7:3). Upon return to room temperature, the mixture was washed twice with 1N aqueous HCl solution (20 mL), and once with saturated aqueous $NaHCO_3$ solution (50 mL) and brine (20 mL). The organic layer was dried over anhydrous Na_2SO_4 and the solvent was evaporated under reduced pressure and the crude product was purified by column chromatography to obtain bis-β-lactams **16a–g** (see the Supplementary Information for details).

2-(2-(Anthracen-9-yl)-1-(4-ethoxyphenyl)-4-oxoazetidin-3-yl)-7-(2-(anthracen-9-yl)-1-(4-ethoxyphenyl)-4-oxoazetidin-3-yl)benzo[*lmn*][3,8]phenanthroline-1,3,6,8(2*H*,7*H*)-tetraone (16a)

Brown solid (Yield 60%); Mp. 145–147 °C; IR (KBr, cm $^{-1}$): 1751 (CO β-lactam), 1705 (CO Naph), 1674 (CO Naph); ^{1}H NMR (250 MHz, DMSO-d_6) δ 1.27)6H, *t*, J = 7.0 Hz, $2CH_3$), 3.81 (4H, *q*, J = 7.0 Hz, $2O\text{-}CH_2$), 6.71–6.86 (6H, *m*, H-4 β-lactam, ArH), 6.95 (2H, *d*, J = 2.2 Hz, H-3 β-lactam), 7.08 (4H, *d*, J = 8.7 Hz, ArH), 7.45–7.66 (8H, *m*, ArH), 8.16 (4H, *d*, J = 7.5 Hz, ArH), 8.46–8.55 (4H, *m*, ArH), 8.63 (4H, *s*, ArH), 8.74 (2H, *s*, ArH); ^{13}C NMR (100 MHz, DMSO-d_6) δ 163.1 (CO β-lactam), 162.2 (CO Naph), 155.6, 132.0, 131.6, 131.4, 131.1, 130.6, 129.1, 128.1, 126.9, 126.8, 125.7, 121.0, 118.3, 115.5, 114.9 (aromatic carbons), 63.6 ($O\text{–}CH_2$), 62.7 (C-3 β-lactam), 56.1 (C-4 β-lactam), 15.0 (CH_3); Analysis calculated for $C_{64}H_{44}N_4O_8$: C, 77.10; H, 4.45; N, 5.62%. Found: C, 77.02; H, 4.25; N, 5.45%.

2-(2-(Anthracen-9-yl)-1-(4-methoxyphenyl)-4-oxoazetidin-3-yl)-7-(2-(anthracen-9-yl)-1-(4-methoxyphenyl)-4-oxoazetidin-3-yl)benzo[*lmn*][3,8]phenanthroline-1,3,6,8 (2*H*,7*H*)-tetraone (16b)

Brown solid (Yield 55%); Mp. 159–161 °C; IR (KBr, cm $^{-1}$): 1759 (CO β-lactam), 1712 (CO Naph), 1674 (CO Naph); ^{1}H NMR (250 MHz, DMSO-d_6) δ 3.57)6H, *s*, $O\text{–}CH_3$), 6.71 (2H, *d*, J = 2.5 Hz, H-4 β-lactam), 6.76 (4H, *d*, J = 9.0 Hz, ArH), 6.95 (2H, *d*, J = 2.5 Hz, H-3 β-lactam), 7.09 (4H, *d*, J = 9.0 Hz, ArH), 7.50–7.58 (8H, *m*, ArH), 8.17 (4H, *d*, J = 8.0 Hz, ArH), 8.48–8.54 (4H, *m*, ArH), 8.63 (4H, *s*, ArH), 8.74 (2H, *s*, ArH); ^{13}C NMR (100 MHz, DMSO-d_6) δ 163.1 (CO β-lactam), 162.3 (CO Naph), 159.4, 131.5, 131.2, 130.7, 129.8, 128.1, 127.2, 126.9, 126.8, 126.3, 125.7, 124.3, 118.9, 118.3, 115.1 (aromatic carbons), 62.8 (C-3 β-lactam), 56.1 (C-4 β-lactam), 55.6 ($O\text{–}CH_3$); Analysis calculated for $C_{62}H_{40}N_4O_8$: C, 76.85; H, 4.16; N, 5.78%. Found: C, 76.78; H, 4.10; N, 5.62%.

2-(2-(Anthracen-9-yl)-1-(4-(dimethylamino)phenyl)-4-oxoazetidin-3-yl)-7-(2-(anthracen-9-yl)-1-(4-(dimethylamino)phenyl)-4-oxoazetidin-3-yl)benzo[*lmn*][3,8] phenanthroline-1,3,6,8(2*H*,7*H*)-tetraone (16c)

Green solid (Yield 45%); Mp. 150–152 °C; IR (KBr, cm^{-1}): 1759 (CO β-lactam), 1712 (CO Naph), 1674 (CO Naph); ^{1}H NMR (250 MHz, DMSO-d_6) δ 2.70)12H, *s*, $N\text{–}CH_3$), 6.52 (4H, *d*, J = 8.7 Hz, ArH), 6.63 (2H, *d*, J = 2.7 Hz, H-4 β-lactam), 6.68 (2H, *d*, J = 2.7 Hz, H-3 β-lactam) 7.01 (4H, *d*, J = 8.7 Hz, ArH), 7.49–7.61 (8H, *m*, ArH), 8.15 (4H, *d*, J = 8.2 Hz, ArH), 8.49–8.57 (4H, *m*, ArH), 8.63 (4H, *s*, ArH), 8.73 (2H, *s*, ArH); ^{13}C NMR (100 MHz, DMSO-d_6) δ 163.4 (CO β-lactam), 162.2 (CO Naph), 146.9, 135.7, 131.4, 130.4, 129.5, 127.4, 126.3, 122.7, 120.8, 118.2, 117.8, 115.3, 115.1, 114.0, 112.8 (aromatic carbons), 63.9 (C-3 β-lactam), 57.5 (C-4 β-lactam), 40.0 ($N\text{–}CH_3$); Analysis calculated for $C_{64}H_{46}N_6O_6$: C, 77.25; H, 4.66; N, 8.45%. Found: C, 77.08; H, 4.60; N, 8.12%.

2-(2-(Anthracen-9-yl)-1-(4-(diethylamino)phenyl)-4-oxoazetidin-3-yl)-7-(2-(anthracen-9-yl)-1-(4-(diethylamino) phenyl)-4-oxoazetidin-3-yl)benzo[*lmn*][3,8]phenanthroline-1,3,6,8(2*H*,7*H*)-tetraone (16d)

brown solid (Yield 40%); Mp. 148–150 °C; IR (KBr, cm^{-1}): 1751 (CO β-lactam), 1712 (CO Naph), 1674 (CO Naph); ^{1}H NMR (250 MHz, DMSO-d_6) δ 1.37)12H, *t*, J = 6.7 Hz, CH_3), 3.96)8H, *q*, J = 6.7 Hz, $N\text{–}CH_2$), 6.48 (4H, *d*, J = 5.0 Hz, ArH), 6.71 (2H, *d*, J = 2.5 Hz, H-4 β-lactam), 6.94 (2H, *d*, J = 2.5 Hz, H-3 β-lactam), 7.01 (4H, *d*, J = 5.0 Hz, ArH), 7.54–7.68 (8H, *m*, ArH), 8.19 (4H, *d*, J = 5.0 Hz, ArH),

8.53–8.54 (4H, *m*, ArH), 8.66 (4H, *s*, ArH), 8.76 (2H, *s*, ArH); ^{13}C NMR (100 MHz, DMSO-d_6) δ 163.1 (CO β-lactam), 161.6 (CO Naph), 145.1, 144.6, 135.9, 135.3, 133.0, 132.5, 131.6, 130.4, 128.0, 126.9, 126.8, 121.3, 118.7, 113.0, 112.3, (aromatic carbons), 62.6 (C-3 β-lactam), 55.8 (C-4 β-lactam), 44.0 (–NCH_2), 12.8 (CH_3); Analysis calculated for $C_{68}H_{54}N_6O_6$: C, 77.70; H, 5.18; N, 7.99%. Found: C, 76.98; H, 4.95; N, 7.52%.

2-(2-(3,4-Dimethoxyphenyl)-1-(4-ethoxyphenyl)-4-oxoazetidin-3-yl)-7-2-(3,4-dimethoxyphenyl)-1-(4-ethoxyphenyl)-4-oxoazetidin-3-yl)benzo[*lmn*][3,8]phenanthroline-1,3,6,8(2*H*,7*H*)-tetraone (16e)

Light brown solid (Yield 65%); Mp. 146–148 °C; IR (KBr, cm^{-1}): 1759 (CO β-lactam), 1712 (CO Naph), 1674 (CO Naph); ^{1}H NMR (250 MHz, DMSO-d_6) δ 1.28)6H, *t*, J = 7.0 Hz, CH_3), 3.69)6H, *s*, O–CH_3), 3.73)6H, *s*, O–CH_3), 3.95)4H, *q*, J = 7.0 Hz, O–CH_2), 5.42 (2H, *d*, J = 2.5 Hz, H-4 β-lactam), 5.94 (2H, *d*, J = 2.5 Hz, H-3 β-lactam), 6.90 (4H, *d*, J = 9.0 Hz, ArH), 6.94 (2H, *d*, J = 8.5 Hz, ArH), 7.05 (2H, *d*, J = 8.7 Hz, ArH), 7.16–7.22 (6H, *m*, ArH), 8.68 (4H, *s*, ArH); ^{13}C NMR (100 MHz, DMSO-d_6) δ 162.9 (CO β-lactam), 162.8 (CO Naph), 155.4, 149.4, 132.1, 131.4, 131.2, 129.3, 129.1, 126.8, 119.6, 118.9, 115.4, 112.3, 111.0 (aromatic carbons), 64.2 (O–CH_2), 63.7 (C-3 β-lactam), 59.5 (C-4 β-lactam), 56.0 (O–CH_3), 55.9 (O–CH_3), 15.1 (CH_3); Analysis calculated for $C_{52}H_{44}N_4O_{12}$: C, 68.11; H, 4.84; N, 6.11%. Found: C, 68.01; H, 4.65; N, 5.92%.

2-(2-(3,4-Dimethoxyphenyl)-1-(4-(dimethylamino)phenyl)-4-oxoazetidin-3-yl)-7-(-2-(3,4-dimethoxyphenyl)-1-(4-(dimethylamino)phenyl)-4-oxoazetidin-3-yl)benzo[*lmn*][3,8]phenanthroline-1,3,6,8(2*H*,7*H*)-tetraone (16f)

Dark green solid (Yield 47%); Mp. 165–167 °C; IR (KBr, cm^{-1}): 1766 (CO β-lactam), 1712 (CO Naph), 1674 (CO Naph); ^{1}H NMR (250 MHz, DMSO-d_6) δ 2.82)12H, *s*, *N*–CH_3), 3.69)6H, *s*, O–CH_3), 3.72)6H, *s*, O–CH_3), 5.42 (2H, *d*, J = 2.2 Hz, H-4 β-lactam), 5.91 (2H, *d*, J = 2.2 Hz, H-3 β-lactam), 6.69 (4H, *d*, J = 8.5 Hz, ArH), 6.94 (2H, *d*, J = 11.0 Hz, ArH), 7.03 (2H, *d*, J = 8.0 Hz, ArH), 7.11–7.15 (6H, *m*, ArH), 8.69 (4H, *s*, ArH); ^{13}C NMR (100 MHz, DMSO-d_6) δ 163.1 (CO β-lactam), 162.8 (CO Naph), 155.4, 149.4, 147.6, 131.4, 131.2, 129.3, 126.8, 126.5, 119.6, 118.9, 115.4, 112.3, 111.0 (aromatic carbons), 62.7 (C-3 β-lactam), 59.5 (C-4 β-lactam), 56.0 (O–CH_3), 55.9 (O–CH_3), 40.3 (*N*–CH_3); Analysis calculated for $C_{52}H_{46}N_6O_{10}$: C, 68.26; H, 5.07; N, 9.19%. Found: C, 68.18; H, 4.95; N, 8.92%.

2-(1-(4-Methoxyphenyl)-4-oxospiro[azetidine-2,9′-fluoren]-3-yl)-7-((S)-1-(4-methoxyphenyl)-4-oxospiro[azetidine-2,9′-fluoren]-3-yl)benzo[*lmn*][3,8]phenanthroline-1,3,6,8(2*H*,7*H*)-tetraone (16g)

Dark orang solid (Yield 68%); Mp. 159–161 °C; IR (KBr, cm^{-1}): 1766 (CO β-lactam), 1712 (CO Naph), 1681 (CO Naph); ^{1}H NMR (250 MHz, DMSO-d_6) δ 3.60)6H, *s*, O–CH_3), 6.15 (2H, *s*, H-3 β-lactam), 6.76 (4H, *d*, J = 8.8 Hz, ArH), 6.85 (4H, *d*, J = 8.8 Hz, ArH), 7.02–7.06 (2H, *m*, ArH), 7.27–7.31 (2H, *m*, ArH), 7.40–7.53 (6H, *m*, ArH), 7.73 (2H, *d*, J = 7.2 Hz, ArH), 7.87–7.95 (4H, *m*, ArH), 8.69 (4H, *s*, ArH); ^{13}C NMR (100 MHz, DMSO-d_6) δ 162.4 (CO β-lactam), 160.4 (CO Naph), 156.3, 143.3, 141.7, 139.5, 138.1, 130.5, 130.3, 129.0, 126.4, 123.3, 121.5, 118.4, 114.9 (aromatic carbons), 72.7 (C-3 β-lactam), 67.7 (spiro carbon), 55.6 (O–CH_3); Analysis calculated for $C_{58}H_{36}N_4O_8$: C, 75.97; H, 3.96; N, 6.11%. Found: C, 75.78; H, 3.65; N, 5.92%.

DPPH radical scavenging

For evaluating radical scavenging activity, the diphenylpicrylhydrazyl (DPPH) scavenging assay was performed as described previously (Malterud et al. 1993). Briefly, a suitable dilution of test compound (0.05 ml) dissolved in DMSO was mixed with a solution of DPPH in methanol (A_{517} = 1.0; 2.95 ml) and the UV absorbance at 517 nm was measured both before addition of the test lactam and again after 5 min. Percent radical scavenging was calculated as $100 \times (A_{start} - A_{end})/(A_{start})$, where A_{start} is the absorbance before addition of test compound and A_{end} is the absorbance value after 5 min of reaction time. Vitamin C in DMSO (195 µg/ml) and blank DMSO were used as positive and negative controls, respectively.

Method of anticancer activity and cytotoxicity assays

In vitro cytotoxic effect of some compounds was evaluated using standard 3-(4,5-dimethylthiazol-2-yl)-2, 5-diphenyltetrazolium bromide (MTT) assay (Mosmann 1983; Riss et al. 2013; Rowan et al. 2001). The MCF-7 (breast cancer cells), TC-1 (mouse lung epithelial cells), and *HepG2* (liver hepatocellular carcinoma cells) cell lines (all cell lines were purchased from cell culture collection of Pasteur Institute, Tehran branch, Iran) were seeded in 96-well plate at a density of 5×10^3 cells/well. Cells were incubated at 37 °C in humidified 5% CO_2 incubator. After incubation for 24 h, the cells were incubated with 200, 50, 10, and 5 µM concentrations of compounds. After 24 h, the medium was removed and the cells were washed with phosphate buffered saline then, 25 µl of MTT solution (4 µM) was added to each well and incubated at 37 °C for 4 h. After incubation time, The MTT solution was removed

from the wells and replaced with 100 µl of dimethylsulfoxide (DMSO). After 10 mines incubation at 37 °C, the optical absorption was read at a wavelength of 540 nm using a microplate reader (Power wave X52, BioTek instrument Inc., US). All experiments were accomplished in triplicate for each concentration (Kianpour et al. 2017, 2018)

UV–visible and fluorescence spectroscopy

Calf thymus DNA (CT-DNA) was purchased from Sigma-Aldrich and used without further purification. UV–vis spectra were obtained using a Perkin-Elmer Lambda 25 spectrophotometer. Temperature was controlled by a EYELA NCB-3100 constant temperature bath. Fluorescence determination was recorded on an LS45 spectrofluorimeter equipped with thermostat bath and quartz cells (1.0 cm). Experiments were done in 50 mM Tris-HCl buffer containing 100 mM NaCl at pH 7.4. CT-DNA solution was prepared with doubly distilled water, and it was stored at 4 °C in the dark. UV–visible absorption titration studies have been performed using a fixed concentration of the compounds (**16a**, **16b**, and **16e** (20 µM), **16d** (28 µM), **16f** (40 µM), and **16g** (62 µM) all in DMSO) and varying the CT-DNA concentration. The concentration of CT-DNA was determined by UV–vis absorption spectroscopy, and the molar extinction coefficient (6600 M^{-1} cm^{-1}) at ~260 nm was obtained (Zsila et al. 2004). The purity of DNA was determined by following the absorption ratio of the bands at 260 and 280 nm. It was found to be 1.8, showing that DNA is sufficiently protein-free (Marmur 1961).

Molecular docking study

In the present study, **16d** was screened for targeted DNA using the AutoDock tools to corroborate the results gathered from spectroscopic measurement (Arif et al. 2020; Arunadevi et al. 2019; Yazdani et al. 2019). The crystal structure of double-stranded DNA (PDB code: 453D, B-DNA [(5′-D(*CP*GP*CP*GP*AP*AP*TP*TP*CP*GP*CP*G)]) were obtained from the protein data bank (http://www.rcsb.org). Interactions between ligands and DNA were studied by AutoDock 4.2. Structures of ligands were sketched and optimized by molecular mechanics using Hyperchem software. The PDBQT files were generated by adding charges and defining the degree of torsions (Iraji et al. 2018). The DNA file was prepared by adding polar hydrogen atom with Gasteiger-Huckel charges and water molecules were removed. Next, the created three-dimensional grids were 60 × 60 × 60 (x, y, z) with a grid spacing of 0.375 Å and the cubic grids were centered on the binding site of native ligand. Lamarckian genetic algorithm was applied to model the interaction/binding between the ligand and duplex. The other parameters were left at program default values. The final binding mode depicted was selected taking into account the best-ranked scoring functions (Shaikh et al. 2017). Ligand DNA interactions were visualized on the basis of docking results using Discovery Studio Visualizer 17.2.

Acknowledgements The authors would like to thank the Shiraz University Research Council for financial support (Grant no. 97-GR-SC-23) and Dr. Attila Benyei for collecting X-ray data.

Compliance with ethical standards

Conflict of interest The authors declare that they have no conflict of interest.

Publisher's note Springer Nature remains neutral with regard to jurisdictional claims in published maps and institutional affiliations.

References

Abdel-Aziz AA-M, ElTahir KEH, Asiri YA (2011) Synthesis, anti-inflammatory activity and COX-1/COX-2 inhibition of novel substituted cyclic imides. Part 1: molecular docking study. Eur J Med Chem 46:1648–1655

Alami N, Paterson J, Belanger S, Juste S, Grieshaber CK, Leyland-Jones B (2007) Comparative analysis of xanafide cytotoxicity in breast cancer cell lines. Br J Cancer 97:58–64

Alborz M, Jarrahpour AA, Pournejati R, Karbalaei-Heidari HR, Sinou V, Latour C, Brunel JM, Sharghi H, Aberi M, Turos E, Wojtas L (2018) Synthesis and biological evaluation of some novel diastereoselective benzothiazole β-lactam conjugates. Eur J Med Chem 143:283–291

Ameri RJ, Jarrahpour A, Latour CH, Sinou V, Brunel JM, Zgou H, Mabkhot Y, Ben Hadda T, Turos E (2017) Synthesis and antimicrobial/antimalarial activities of novel naphthalimido trans-β-lactam derivatives. Med Chem Res 10:2235–2242

Amr AEGE, Sabry NM, Abdulla MM (2007) Synthesis, reactions, and anti-inflammatory activity of heterocyclic systems fused to a thiophene moiety using citrazinic acid as synthon. Monatshefte für Chem Chem Monthly 138:699–707

Anizon F, Belin L, Moreau P, Sancelme M, Voldoire A, Prudhomme M, Ollier M, Severe D, Riou JF, Bailly C, Fabbro D, Thomas M (1997) Syntheses and biological activities (topoisomerase inhibition and antitumor and antimicrobial properties) of rebeccamycin analogues bearing modified sugar moieties and substituted on the imide nitrogen with a methyl group. J Med Chem 21:3456–3465

Arif R, Rana M, Yasmeen S, Khan MS, Abid M, Khan MS (2020) Facile synthesis of chalcone derivatives as antibacterial agents: synthesis, DNA binding, molecular docking, DFT and antioxidant studies. J Mol Struct 1208:127905

Arunadevi A, Porkodi J, Ramgeetha L, Raman N (2019) Biological evaluation, molecular docking and DNA interaction studies of coordination compounds gleaned from a pyrazolone incorporated ligand. Nucleosides Nucleotides Nucleic Acids 38:656–679

Arya N, Jagdale AY, Patil TA, Yeramwar SS, Holikatti SS, Dwivedi J, Shishoo CJ, Jain KS (2014) The chemistry and biological potential of azetidin-2-ones. Eur J Med Chem 74:619–656

Arya S, Kumar S, Rani R, Kumar N, Roy P, Sondhi S (2013) Synthesis, anti-inflammatory, and cytotoxicity evaluation of 9,10-

dihydroanthracene-9,10-α,β-succinimide and bis-succinimide derivatives. Med Chem Res 22:4278–4285

Ayati A, Bakhshaiesh TO, Moghimi S, Esmaeili R, Majidzadeh-A K, Safavi M, Firoozpour L, Emami S, Foroumadi A (2018) Synthesis and biological evaluation of new coumarins bearing 2, 4-diaminothiazole-5-carbonyl moiety. Eur J Med Chem 155:483–491

Banerjee S, Kitchen JA, Gunnlaugsson T, Kelly JM (2013) The effect of the 4-amino functionality on the photophysical and DNA binding properties of alkyl-pyridinium derived 1,8-naphthalimides. Org Biomol Chem 11:5642–5655

Baraldi PG, Preti D, Fruttarolo F, Tabrizi MA, Romagnoli R (2007) Hybrid molecules between distamycin A and active moieties of antitumor agents. Bioorg Med Chem 15:17–35

Baraldi PG, Romagnoli R, Guadix AE, Pineda de las Infantas MJ, Gallo MA, Espinosa A, Martinez A, Bingham JP, Hartley JA (2002) Design, synthesis, and biological activity of hybrid compounds between uramustine and DNA minor groove binder distamycin A. J Med Chem 45:3630–3638

Benzie IFF, Strain JJ (1999) Ferric reducing/antioxidant power assay: direct measure of total antioxidant activity of biological fluids and modified version for simultaneous measurement of total antioxidant power and ascorbic acid concentration. Meth Enzymol 299:15–27

Berlinck RG, Britton R, Piers E, Lim L, Roberge M, Moreira da Rocha R, Andersen RJ (1998) Granulatimide and isogranulatimide, aromatic alkaloids with G2 checkpoint inhibition activity isolated from the Brazilian ascidian *Didemnum granulatum*: structure elucidation and synthesis. J Org Chem 63:9850–9856

Bhat SS, Kumbhar AA, Heptullah H, Khan AA, Gobre VV, Gejji SP, Puranik VG (2010) Synthesis, electronic structure, DNA and protein binding, DNA cleavage, and anticancer activity of fluorophore-labeled copper (II) complexes. Inorg Chem 50:545–558

Borazjani N, Jarrahpour A, Ameri Rad J, Mohkam M, Behzadi M, Ghasemi Y, Mirzaeinia S, Karbalaei-Heidari HR, Ghanbari MM, Batta G, Turos E (2019a) Design, synthesis and biological evaluation of some novel diastereoselective β-lactams bearing 2-mercaptobenzothiazole and benzoquinoline. Med Chem Res 28:329–339

Borazjani N, Sepehri S, Behzadi M, Jarrahpour A, Ameri Rad J, Sasanipour M, Mohkam M, Ghasemi Y, Akbarizadeh AR, Digiorgio C, Brunel JM, Ghanbari MM, Batta G, Turos E (2019b) Three-component synthesis of chromeno β-lactam, Eur. J Med Chem 179:389–403

Cossio FP, Ugalde JM, Lopez X, Lecea B, Palomo C (1993) A semiempirical theoretical study on the formation of β-lactams from ketenes and imines. J Am Chem Soc 115:995–1004

De Oliveira KN, Chiaradia LD, Martins PGA, Mascarello A, Cordeiro MNS, Guido RVC, Andricopulo AD, Yunes RA, Nunes RJ, Vernal J, Terenzi H (2011) Sulfonyl-hydrazones of cyclic imides derivatives as potent inhibitors of the *Mycobacterium tuberculosis* protein tyrosine phosphatase B (PtpB). MedChemComm 2:500–504

El-Azab AS, Alanazi AM, Abdel-Aziz NI, Al-Suwaidan IA, El-Sayed MAA, El-Sherbeny MA, Abdel-Aziz AAM (2013) Synthesis, molecular modeling study, preliminary antibacterial, and antitumor evaluation of *N*-substituted naphthalimides and their structural analogues. Med Chem Res 22:2360–2375

Galletti P, Soldati R, Pori M, Durso M, Tolomelli A, Gentilucci L, Dattoli SD, Baiula M, Spampinato S, Giacomini D (2014) Targeting integrins αvβ3 and α5β1 with new β-lactam derivatives. Eur J Med Chem 83:284–293

Ge C, Chang L, Zhao Y, Chang C, Xu X, He H, Wang Y, Dai F, Xie S, Wang C (2017) Design, synthesis and evaluation of naphthalimide derivatives as potential anticancer agents for hepatocellular carcinoma. Molecules 22:342

Geesala R, Gangasani JK, Budde M, Balasubramanian S, Vaidya JR, Das A (2016) 2-Azetidinones: Synthesis and biological evaluation as potential anti-breast cancer agents. Eur J Med Chem 124:544–558

Gudeika D, Lygaitis R, Gražulevičius JV, Kublickas RH, Rubežienė V, Vedegytė J (2012) Synthesis and properties of dimeric naphthalene diimides. Chemija 23:233–238

Hénon H, Messaoudi S, Anizon F, Aboab B, Kucharczyk N, Léonce S, Golsteyn R, Pfeiffer MB, Prudhomme M (2007) Bis-imide granulatimide analogues as potent checkpoint 1 kinase inhibitors. Eur J Pharm 554:106–112

Iraji A, Firuzi O, Khoshneviszadeh M, Nadri H, Edraki N, Miri R (2018) Synthesis and structure-activity relationship study of multi-target triazine derivatives as innovative candidates for treatment of Alzheimer's disease. Bioorg Chem 77:223–235

Kamal A, Reddy BSN, Reddy GSK, Ramesh G (2002) Design and synthesis of C-8 linked pyrrolobenzodiazepine–naphthalimide hybrids as anti-tumour agents. Bioorg Med Chem Lett 12:1933–1935

Kamboj VK, Kapoor A, Jain S (2019) Synthesis, antimicrobial, and antioxidant screening of aryl acetic acid incorporated 1,2,4-triazolo-1,3,4-thiadiazole derivatives. J Heterocycl Chem 56:1376–1382

Kianpour S, Ebrahiminezhad A, Mohkam M, Tamaddon AM, Dehshahri A, Heidari R, Ghasemi Y (2017) Physicochemical and biological characteristics of the nanostructured polysaccharide-iron hydrogel produced by microorganism *Klebsiella oxytoca*. J Basic Microbiol 57:132–140

Kianpour S, Ebrahiminezhad A, Negahdaripour M, Mohkam M, Mohammadi F, Niknezhad SV (2018) Y. Ghasemi, Characterization of biogenic Fe (III)-binding exopolysaccharide nanoparticles produced by Ralstonia sp. SK03. Biotech Prog 34:1167–76

Kostova I, Bhatia S, Grigorov P, Balkansky S, Parmar VS, Prasad AK, Saso L (2011) Coumarins as antioxidants. Curr Med Chem 18:3929–3951

Kumar Gupta R, Pandey R, Sharma G, Prasad R, Koch B, Srikrishna S, Li PZ, Xu Q, Pandey DS (2013) DNA binding and anti-cancer activity of redox-active heteroleptic piano-stool Ru(II), Rh(III), and Ir(III) complexes containing 4-(2-methoxypyridyl)phenyldipyrromethene. Inorg Chem 52:3687–3698

Kumar A, Banerjee S, Roy P, Sondhi SM, Sharma A (2017) Solvent free, catalyst free, microwave or grinding assisted synthesis of bis-cyclic imide derivatives and their evaluation for anticancer activity. Bioorg Med Chem Lett 27:501–504

Landa A, Mielgo A, Oiarbide M, Palomo C (2018) Asymmetric synthesis of β-lactams by the Staudinger reaction. Organic reactions. John Wiley & Sons, Hobokenpp, p 1–123

Laronze M, Boisbrun M, Leonce S, Pfeiffer B, Renard P, Lozach O, Meijer L, Lansiaux A, Bailly C, Sapi J, Laronzea JY (2005) Synthesis and anticancer activity of new pyrrolocarbazoles and pyrrolo-β-carbolines. Bioorg Med Chem 13:2263–2283

Li Q, Fang H, Wang X, Xu W (2010) Novel cyclic-imide peptidomimetics as aminopeptidase N inhibitors. Structure-based design, chemistry and activity evaluation. Eur J Med Chem 45:1618–1626

Li Y, Li Y, Liu X, Yang Y, Lin D, Gao Q (2020) The synthesis, characterization, DNA/protein interaction, molecular docking and catecholase activity of two Co (II) complexes constructed from the aroylhydrazone ligand. J Mol Struct 1202:127229

Li S, Xu S, Tang Y, Ding S, Zhang J, Wang S, Zhou G, Zhou C, Li X (2014). Synthesis, anticancer activity and DNA-binding properties of novel 4-pyrazolyl-1,8-naphthalimide derivatives. Bioorg Med Chem Lett 24:586–590

Machado KE, de Oliveira KN, Santos-Bubniak L, Licinio MA, Nunes RJ, Santos-Silva MC (2011) Evaluation of apoptotic effect of cyclic imide derivatives on murine B16F10 melanoma cells. Bioorg Med Chem 19:6285–6291

Malterud KE, Farbrot TL, Huse AE, Sund RB (1993) Antioxidant and radical scavenging effects of anthraquinones and anthrones. Pharmacol 47:77–85

Mandegani Z, Asadi Z, Asadi M, Karbalaei-Heidari HR, Rastegari B (2016) Synthesis, characterization, DNA binding, cleavage activity, cytotoxicity and molecular docking of new nano water-soluble $[M(5\text{-}CH_2PPh3\text{-}3,4\text{-}salpyr)](ClO_4)_2$ (M = Ni, Zn) complexes. Dalton Trans 15:6592–6611

Marmur J (1961) A procedure for the isolation of deoxyribonucleic acid from micro-organisms. J Mol Biol 3:208-IN1

Milelli A, Tumiatti V, Micco M, Rosini M, Zuccari G, Raffaghello L, Bianchi G, Pistoia V, Díaz JF, Pera B, Trigili C (2012) Structure–activity relationships of novel substituted naphthalene diimides as anticancer agents. Eur J Med Chem 57:417–428

Miller KD, Siegel RL, Lin CC, Mariotto AB, Kramer JL, Rowland JH, Stein KD, Alteri R, Jemal A (2016) Cancer treatment and survivorship statistics. CA Cancer J Clin 66:271–289

Mondal S, Samajdar RN, Mukherjee S, Bhattacharyya AJ, Bagchi B (2018) Unique eatures of metformin: A combined experimental, theoretical, and simulation study of its structure, dynamics, and interaction energetics with DNA grooves. J Phys Chem B 122:227–2242

Mosmann T (1983) Rapid colorimetric assay for cellular growth and survival: application to proliferation and cytotoxicity assays. J Immunol Methods 65:55–63

Palomo C, Aizpurua JM, Ganboa I, Oiarbide M (2004) Asymmetric synthesis of β-lactams through the Staudinger reaction and their use as building blocks of natural and nonnatural products. Curr Med Chem 11:1837–1872

Parul DM, Sengar NPS, Pathak AK (2010) 2-Azetidinone A new profile of pharmacological activities. Eur J Med Chem 45:5541–5560

Riss TL, Moravec RA, Niles AL, Benink HA, Worzella TJ, Minor L (2013) Cell viability assays, assay guidance manual. Eli Lilly & Company and the National Center for Advancing Translational Sciences, Bethesda, MD, USA, p 1–23

Rowan NJ, Deans K, Anderson JG, Gemmell CG, Hunter IS, Chaithong T (2001) Putative virulence factor expression by clinical and food isolates of Bacillus spp. after growth in reconstituted infant milk formulae. Appl Environ Microbiol 67:3873–3881

Said SA, Amr AEGE, Sabry NM, Abdalla MM (2009) Analgesic, anticonvulsant and anti-inflammatory activities of some synthesized benzodiazipine, triazolopyrimidine and bis-imide derivatives. Eur J Med Chem 44:4787–4792

Shaikh SKJ, Kamble RR, Somagond SM, Devarajegowda HC, Dixit SR, Joshi SD (2017) Tetrazolylmethyl quinolines: Design, docking studies, synthesis, anticancer and antifungal analyses. Eur J Med Chem 128:258–273

Suh D, Chaires JB (1995) Criteria for the mode of binding of DNA binding agents. Bioorg Med Cehm 3:723–728

Tomczyk MD, Walczak KZ (2018) l,8-Naphthalimide based DNA intercalators and anticancer agents. A systematic review from 2007 to 2017. Eur J Med Chem 159:393–422

Tumiatti V, Milelli A, Minarini A, Micco M, Gasperi Campani A, Roncuzzi L, Baiocchi D, Marinello J, Capranico G, Zini M, Stefanelli C (2009) Design, synthesis, and biological evaluation of substituted naphthalene imides and diimides as anticancer agent. J Med Chem 52:7873–7877

Wang LJ, Geng CA, MA YB, Luo J, Huang XY, Chen H, Zhou NJ, Zhang XM, Chen JJ (2012) Design, synthesis, and molecular hybrids of caudatin and cinnamic acids as novel anti-hepatitis B virus agents. Eur J Med Chem 54:352–365

Westrip SP (2010) publCIF: Software for editing, validating and formatting crystallographic information files. J Appl Crys 43:920–925

Xiao H, Chen M, Shi G, Wang L, Yin H, Mei C (2010) A novel fluorescent molecule based on 1, 8-naphthalimide: synthesis, spectral properties, and application in cell imaging. Res Chem Intermed 36:1021–1026

Yazdani M, Edraki N, Badri R, Khoshneviszadeh M, Iraji A, Firuzi O (2019) Multi-target inhibitors against Alzheimer disease derived from 3-hydrazinyl 1, 2, 4-triazine scaffold containing pendant phenoxy methyl-1, 2, 3-triazole: Design, synthesis and biological evaluation. Bioorg Chem 84:363–371

Zanoza SO, Klimenko KO, Maltzev GV, Bykova TI, Levandovskiy IA, Lyakhov SA (2019) Aminoalkoxyfluorenones and aminoalkoxybiphenyls: DNA binding modes. Bioorg Chem 86:52–60

Zhang G, Shen J, Cheng H, Zhu L, Fang L, Luo S, Muller MT, Lee GE, Wei L, Du Y, Sun D (2005) Syntheses and biological activities of rebeccamycin analogues with uncommon sugars. J Med Chem 48:2600–2611

Zsila F, Bikádi Z, Simonyi M (2004) Circular dichroism spectroscopic studies reveal pH dependent binding of curcumin in the minor groove of natural and synthetic nucleic acids. Org Biomol Chem 2:2902–2910